NASA TECHNICAL MEMORANDUM

NASA TM X-3260

NASA TM X-3260

DESIGN AND EVALUATION OF A SENSOR FAIL-OPERATIONAL CONTROL SYSTEM FOR A DIGITALLY CONTROLLED TURBOFAN ENGINE

Frank J. Hrach, Dale J. Arpasi, and William M. Bruton

Lewis Research Center
Cleveland, Ohio 44135

NATIONAL AERONAUTICS AND SPACE ADMINISTRATION • WASHINGTON, D. C. • DECEMBER 1975

1. Report No.	2. Government Accession No.	3. Recipient's Catalog No.
NASA TM X-3260		

4. Title and Subtitle	5. Report Date
DESIGN AND EVALUATION OF A SENSOR FAIL-OPERATIONAL CONTROL SYSTEM FOR A DIGITALLY CONTROLLED TURBOFAN ENGINE	December 1975
	6. Performing Organization Code

7. Author(s)	8. Performing Organization Report No.
Frank J. Hrach, Dale J. Arpasi, and William M. Bruton	E-8401
	10. Work Unit No. 505-05

9. Performing Organization Name and Address	11. Contract or Grant No.
Lewis Research Center National Aeronautics and Space Administration Cleveland, Ohio 44135	

12. Sponsoring Agency Name and Address	13. Type of Report and Period Covered
National Aeronautics and Space Administration Washington, D. C. 20546	Technical Memorandum
	14. Sponsoring Agency Code

15. Supplementary Notes

16. Abstract

A self-learning, sensor fail-operational, control system for the TF30-P-3 afterburning turbofan engine was designed and evaluated. The sensor fail-operational control system includes a digital computer program designed to operate in conjunction with the standard TF30-P-3 bill-of-materials control. Four engine measurements and two compressor face measurements are tested. If any engine measurements are found to have failed, they are replaced by values synthesized from computer-stored information. The control system was evaluated by using a real-time, nonlinear, hybrid-computer engine simulation at sea-level static condition, at a typical cruise condition, and at several extreme flight conditions. Results indicate that the addition of such a system can improve the reliability of an engine digital control system.

17. Key Words (Suggested by Author(s))	18. Distribution Statement
Digital control Control systems Fail-operational Turbofan engine Hybrid computer simulation	Unclassified - unlimited STAR Category 07 (rev.)

19. Security Classif. (of this report)	20. Security Classif. (of this page)	21. No. of Pages	22. Price*
Unclassified	Unclassified	46	$3.75

* For sale by the National Technical Information Service, Springfield, Virginia 22161

DESIGN AND EVALUATION OF A SENSOR FAIL-OPERATIONAL CONTROL SYSTEM FOR A DIGITALLY CONTROLLED TURBOFAN ENGINE

by Frank J. Hrach, Dale J. Arpasi, and William M. Bruton

Lewis Research Center

SUMMARY

A sensor fail-operational digital control system for the TF30-P-3 afterburning turbofan engine was designed and evaluated. The system has the capability of storing (learning) engine operational data when the engine measurements are valid. Four engine measurements, corrected to compressor face conditions, are tested for catastrophic sensor failure. Any valid measurements are replaced with estimates obtained from the valid measurements and tables of operational data previously stored in the computer memory. Data are stored for the engine bleed settings and for both steady-state and acceleration dynamic conditions. The compressor face measurements are tested for any unrealistic variations because the procedure is based upon these signals being correct.

The sensor fail-operational system consists of (1) a digitalization of the standard bill-of-materials (BOM) control for the TF30-P-3 engine and (2) a separate sensor fail-operational digital computer program written especially for the BOM control. It is not a completely new control system designed specifically to incorporate fail-operational requirements.

The system was evaluated on a real-time, nonlinear, hybrid-computer simulation of the TF30-P-3 turbofan engine. Flight conditions examined were sea-level static condition, a typical cruise condition, and several extreme flight conditions.

The study indicates that acceptable control over the range of flight conditions examined is possible with certain levels of sensor failure. For nonafterburning operation, acceptable control is possible even after three of the four engine sensors have failed. For afterburning operation, adequate control can be achieved with no more than a single failure and then only if a modest rate limit is imposed upon engine acceleration. Acceptable control means that none of the engine operating limits have been exceeded and that nearly the same engine thrust performance is achieved.

This work indicates that it is possible to design a sensor fail-operational control system for an aircraft engine which will improve the engine's reliability.

INTRODUCTION

The state of the art of digital computers qualified for aircraft use has advanced to the point where they are now being applied to engine control. A supervisory digital control system is already in use on the advanced military F100-PW-100 engine. For aircraft engine control, as in other control applications, digital control offers some attractive potential benefits. They include lower initial cost; lower maintenance costs; and the ability to implement more accurate control, resulting in improved engine performance. Also digital control offers the capability of easily changing a control mode by simply reprogramming the computer or of modifying the existing control mode during operation by a higher-level adaptive control loop. New engine designs are becoming more complex and require more complex control; and the interaction between airframe, inlet, and propulsion system is becoming more critical for newer aircraft designs. Future control systems must have the capability of providing these complex control functions and of integrating the control of interacting components. A digital control system has this capability.

For digital control to be viable, steps must be taken to ensure that the reliability of full-authority, flight-qualified, digital propulsion control systems approaches that of the well-proved hydromechanical systems presently used on aircraft engines. This applies to the entire system, which includes sensors, effectors, and the digital computer. Reliability can be improved, of course, by means of redundancy for all the elements of the control system. In the digital computer, self-testing and redundancy can be incorporated relatively easily. However, using redundant sensors and effectors may not be practical. An alternative approach for handling failures of these elements is fail-operational control. Essentially, this approach involves using a model of the system to provide information necessary for control in the event of a failure. (Of course, this approach can also be used in conjunction with redundancy.)

This report is concerned with sensor failures only and describes the design of a control system which would continue to function adequately even though some engine measurements normally needed for control were not available. A control system of this type is herein referred to as a sensor fail-operational control system. The goal of this and any fail-operational control system is to achieve system performance within acceptable limits for as many failures as possible.

Some theoretical work has been done in the field of fail-operational control. A rather extensive treatment is contained in reference 1. That research develops methods of self-reorganization which can provide a complex linear dynamic system with the ability to restructure itself to compensate for failures in the effectors and sensors and for changes in the linear dynamics. The approach taken is to identify the failure or change in the system and use that information to restructure a feedback control loop to maintain closed-loop stability if possible.

A different approach is taken in reference 2, which is concerned only with sensor failures in an aircraft flight control system. The innovations from a bank of Kalman filters are used to detect sensor failures by means of M-ary hypothesis testing. The detection logic then selects the optimal state estimate from the bank of Kalman filters. Capabilities of the method are demonstrated by a real-time linear simulation of the system with noisy sensors.

The design of a sensor fail-operational control system for a two-spool turbofan engine is presented in reference 3. Ten estimates of each critical engine variable are made by using sensor measurements and a multivariable linearized engine model. The differences between estimates provides the basis for identifying any sensors that have failed. A weighted average of valid estimates is used for control. Corrected engine measurements were used, which permitted the same model to be used for all flight conditions. This system was checked out on a nonlinear digital simulation of the engine.

In reference 4 a sensor fail-operational control system was designed and tested on an actual turbojet engine in a sea-level test stand. The relation between two sensor measurements was stored in a digital computer during normal engine operation. When either sensor failed, an estimate obtained from the valid sensor measurement and the stored relation was used to successfully control the engine. The engine tested was a single-spool J85 turbojet. A limitation of that work was that only a single operating condition (sea-level static) could be examined.

The present work is an extension of that reported in reference 4. In the present study, a wide range of flight conditions is investigated, rather than a single flight condition. Corrected engine variables are used to handle the wide variations in the engine measurements. The present work is done for a more advanced engine, a two-spool turbofan engine, the TF30-P-3. Also, four engine variables are tested, not two as was done in reference 4. Instead of testing the sensor fail-operational system on an actual engine, a real-time nonlinear hybrid computer simulation was used. It is felt that the engine simulation models the engine with sufficient accuracy to permit evaluation of the control system. With an engine simulation, a wide range of flight conditions can be examined relatively easily without the need for an elaborate test facility.

As was done in reference 4, relations between the engine measurements are stored in the digital computer during normal operation. Now, however, the measurements are in corrected variable form. Estimates for any erroneous measurements are made in a manner similar to that of reference 4. With this approach, the sensor fail-operational system can be thought of as storing an algebraic model of the engine under normal control. It assumes that unique relations exist between the measured engine variables. This is true for a particular engine geometry and operating condition. If the relations between the measurements change significantly with configuration (such as bleed settings) and dynamic condition (steady state or transient), it is necessary to store data for each case. This task is well suited for a digital computer because of its large mem-

ory capacity. Here actual nonlinear functions relating the corrected engine measurements are stored, whereas in reference 3 only linear approximations of the relations are made.

The report first describes the system used in the evaluation of the sensor fail-operational system that was developed. It then discusses the concept in general terms. Following this, the application of the concept to the TF30-P-3 engine is described. Finally, the results obtained with the sensor fail-operational system are presented.

TF30-P-3 ENGINE AND CONTROL

Engine

A schematic representation of the TF30-P-3 engine with station designations is presented in figure 1. The TF30-P-3 engine is a two-spool, mixed-flow, afterburning turbofan engine. A three-stage, axial-flow fan is mounted on the same shaft with a six-stage, axial-flow, low-pressure compressor driven by a three-stage, low-pressure turbine. A seven-stage, axial-flow, high-pressure compressor is driven by a single-stage, air-cooled, high-pressure turbine. The engine has a hydraulically actuated, variable-area exhaust nozzle which changes area only during afterburning. The afterburner fuel spray-rings are arranged in five separate afterburning zones. There are two compressor bleeds: a seventh-stage bleed on the low-pressure compressor and a twelfth-stage bleed on the high-pressure compressor.

The variables used for control of the TF30-P-3 are listed in table I under the categories of command input, flight condition, measured compressor face, measured engine, manipulated, and controlled variables. Reference 5 includes a rather detailed description of the operation of the control system. In the present report, it is sufficient to point out that the main fuel flow is determined by two measured engine variables: the high-pressure-rotor speed and the high-pressure-compressor discharge static pressure (which is approximately equal to the combustor pressure). The afterburner fuel flow and the exhaust nozzle area are determined by three measured engine variables: high-pressure-rotor speed, high-pressure-compressor discharge static pressure, and nozzle total pressure. The seventh-stage-bleed position is determined by the inlet Mach number; the twelfth-stage-bleed position is a function of the low-pressure-compressor discharge static pressure and the compressor face total pressure.

The operating limits for the engine which determine the range of the compressor face variables are presented in figure 2. These limits are based upon standard-day conditions and a MIL-E-5008B inlet pressure recovery. The extreme values of compressor face total temperature and pressure are noted on the figure. Note the more than 2:1 variation in total temperature and the 30:1 variation in total pressure. (Symbols are defined in the appendix.)

Engine and Inlet Simulation

The TF30-P-3 engine with a standard inlet has been simulated by using the Lewis Research Center's analog and hybrid computing facility. The simulation, which operates in real time, is described in reference 6. It consists of a fully dynamic representation of the engine but only a steady-state representation of an inlet with a standard MIL-E-5008 B pressure recovery.

The simulation is done on the Electronic Associates, Inc. (EAI) Model 690 Hybrid Computing System, which consists of an EAI 640 Digital Computer, an EAI 693 Hybrid Interface Unit, and an EAI 680 Analog Computer. Two EAI 231-R Analog Computers are also used. Figure 3 illustrates the split of the computational load among the various computers. The split is based on the computing equipment complement of each console and a desire to minimize trunking. The bulk of the calculations are performed on the EAI 680 and the two 231-R Analog Computers. The analog computers perform all the operations characteristic of analog machines (i.e., summing, integration with respect to time, multiplication, attenuation, univariate function generation, etc.). The use of peripheral equipment such as x-y plotters and strip-chart recorders allows continuous user monitoring of computed variables. All the required analog computers are tied together by means of a Centralized Trunk System to allow the transmittal of information between analog consoles.

The 640 Digital Computer is used primarily to perform the bivariate function generation associated with fan, compressor, and turbine performance. The digital computer also provides teletypewriter output listings of selected engine variables. In order to minimize the core storage requirements and digital cycle time, scaled-fraction variables and arithmetic routines are used in the digital program. Scaled-fraction variables are limited to values between ±1. The use of scaled fractions necessitates the scaling of digital variables in the same manner as the analog variables are scaled.

The digital portion of the simulation requires approximately 10 000 words of core storage. The resulting digital sampling interval (with steady analog inputs) is about 4.65 milliseconds, which allows real-time simulation of engine dynamics. The analog portion of the TF30-P-3 hybrid simulation performs all the required computations except the bivariate function generation previously discussed. The analog computational load is split between the 680 Analog Computer and two 231-R Analog Computers. Approximately 185 amplifiers and 85 multipliers are required to perform the analog calculations. The 680 Analog Computer also serves as the interface between the engine simulation and the digital engine controller. The manipulated variables for the engine simulation are provided by an independent digital computer representation of the TF30-P-3 hydromechanical control system described in the next section.

Digital Engine Control

A digitalization of the TF30-P-3 bill-of-materials (BOM) control has been developed for use on the Lewis Research Center's digital computer control facility for on-line control of airbreathing propulsion systems. This digital computer program has been used successfully to control the engine and inlet simulation just described. A detailed description of the program and the results obtained with it are given in reference 5. The digital computer program requires only about 5000 words of the 16 000-word memory available in the facility. Calculation time is as short as 3.2 milliseconds. The matter of necessary sampling time for acceptable control is also investigated in reference 5 and in an earlier report, reference 7. Both these studies indicate that a sampling interval time as long as 50 milliseconds is acceptable. A value of 25 milliseconds was selected for this study. Accurately modeling the hydromechanical control requires that the effect of dynamics for fuel lines and control actuators be taken into account. Two small analog computers are used to model the dynamic relations of these components.

The unused digital control computer memory and the available calculation time are used for the sensor fail-operational computer program. This is described in the section IMPLEMENTATION ON THE TF30-P-3 ENGINE.

The Lewis Research Center's digital computer control facility, which is described in reference 8, was also used in the earlier sensor fail-operational work conducted at Lewis (ref. 4). The heart of the system is a Systems Engineering Laboratories (SEL) Model 810B process control computer with a basic 16 000-word memory.

Table II (extracted from ref. 8) lists some of the digital system capabilities. The computer and its associated equipment are not flight-qualified hardware. However, characteristics such as cycle time, memory, and interrupt structure are typical of what may exist in some future flight system.

A diagram of the complete system used in the sensor fail-operational study is presented in figure 4. The variables transferred to the system and between the components are indicated on the diagram.

SENSOR FAIL-OPERATIONAL CONTROL

Conceptual Basis

Sensor fail-operational control is based on the fact that for a given engine geometry and dynamic condition the same relations exist between certain corrected engine variables over a wide range of power settings and flight conditions. An example of these relations is an operating line on a corrected-variable compressor map, shown schematically in figure 5. As indicated in the figure, throttle setting determines a point on

the operating line. At that point, a unique relation exists between the variables on the map: pressure ratio, corrected engine speed, and corrected airflow. If one variable, for example, pressure ratio, is unavailable, it can be estimated from either of the other two variables at the operating point - from corrected speed, for example. This estimation can be carried out on a digital computer by first storing the relation between these two variables along the operating line.

In the compressor map example, a change in engine geometry, such as a bleed opening, causes a shift of the operating line. It is necessary therefore to store additional relations between the variables for those engine configurations for which the change in the operating line is significant. Also, the locus of operating points during acceleration of the engine shifts toward the surge line. Data for both steady state and acceleration may have to be stored if the shift is large.

The measured engine variables are corrected by the compressor face conditions of total temperature and pressure. They are corrected as indicated in reference 9, rather than being made dimensionless.

Incorporation in an Engine Control System

The sensor fail-operational concept might be made part of an engine control system, as illustrated in figure 6. In this figure, a conventional control system is compared with a system having sensor fail-operational capability, herein called a sensor fail-operational control system. In the conventional control system, the command input, flight condition, measured compressor face, and measured engine variables go directly to the engine control. In a possible sensor fail-operational control system, all these variables except the flight condition variables go to a separate digital program which performs the following functions:

(1) Stores the corrected engine measurements during normal operation for all significant engine configurations and dynamic conditions

(2) After sufficient data are stored, continuously checks the engine measurements to determine whether any are invalid because of a failed sensor

(3) In case of a failure, provides an estimate for the invalid measurement based on the valid measurements and the data stored in the computer for the particular engine geometry and dynamic condition

The system may have a learning capability; that is, data are stored as the engine is operated. This is not an essential feature. Nominal engine operational data could be stored in the computer before startup. Another possibility would be to store the nominal data before startup and to modify these data either by replacing the nominal data with the current data or by averaging the current data with previous data.

A sensor failure is defined as a failure in the transducer itself, in the device which converts the measurement to digital form (which can be part of the transducer), or in the link between the transducer and the computer. Detection of a sensor failure can be a difficult task. Some types, such as a catastrophic failure (hard failure), which is characterized by a sudden change to some unrealistic value, are easy to detect. Others, such as a slow change (soft failure) to some value still within the allowable operating range, are difficult to detect.

In estimating the value of a particular failed measured variable, some of the valid measurements are better to use than others because some variables are more closely coupled together. When possible, it is better to use a closely coupled variable to estimate a value for an invalid measurement.

IMPLEMENTATION ON THE TF30-P-3 ENGINE

A sensor fail-operational digital computer program was written for the TF30-P-3 engine. Features of this program are described in this section.

Learning Procedure

Engine operational data were stored (or learned) as the simulated engine was operated over its complete range. The procedure consisted of varying power lever angle from idle to full afterburning for all three possible bleed settings. Bleeds were operated manually for this initial learning. The variations were at two rates: slow, to approximate a series of steady-state operating points; and rapid (throttle slam), to obtain acceleration data.

Data were not stored during deceleration. It was found that separate data for engine deceleration were not needed; the steady-state data were adequate for estimating values during deceleration.

This procedure may not be practical for the actual engine. As was pointed out previously, it might be better to store nominal engine operational data in the computer before engine startup. This would eliminate the necessity of extensive operation of the engine before flight. The matter of initially getting the data in the computer is an operational problem and is considered to be beyond the scope of this report.

The tables of stored measured engine variables are listed in table III. The relations between each pair of the six possible pairs formed from four corrected measured engine variables are stored. Each table is divided into three parts, the data occupying each part corresponding to one of the three possible bleed setting combinations. Each separate part was allocated 64 words of core storage.

The data are stored as follows: The range of each independent variable in each table was first subdivided into equal increments. The increment end values are called subdivision points. The computer cycles and samples values of the variables to be stored. When a measured value of an independent variable is within 20 percent of one of the subdivision points, the associated value of the dependent variable is taken as the value corresponding to that subdivision point. For each subdivision point, values are simply averaged until 32 samples have been taken; thereafter, a weighted average is taken. The current stored value is weighted by a factor of 31/32, and the present sampled value by a factor of 1/32. This feature of updating the stored data allows for the slow degradation of engine performance but unfortunately also includes the effect of slow degradation of the sensors, an effect it would be desirable to eliminate.

In order to fill any locations (subdivision points) for which no measurements have been made, a linear interpolation scheme is used. In addition, the data are extrapolated beyond the upper and lower values corresponding to the upper and lower values of power lever angle. This is done by extending straight-line segments beyond the learned data. The slopes of the line segments are determined from the maximum and minimum points.

Failure Tests

During the learning phase of operation, failure tests of only the command input and the compressor face variables are made. No failure tests of engine measurements are made until operational data for all bleed settings and both dynamic conditions have been learned over the complete range of power settings. (This is important only if the data are learned during operation and not if nominal engine data are initially stored in the computer.) The variables tested are the command input variable (power lever angle), the measured compressor face variables (total temperature and total pressure), and the measured engine variables (corrected high-pressure-rotor speed, corrected high-pressure-compressor discharge static pressure, corrected low-pressure-compressor discharge static pressure, corrected nozzle total pressure, and nozzle area). The flight condition variables (Mach number and ambient pressure) come from the inlet control and are assumed to be always correct; they are therefore not tested.

The commanded value of power lever angle is directed to the sensor fail-operational computer program because under some conditions the program substitutes a different value than commanded. Although steps will be taken to assure the reliability of this input variable, a test is made to further assure its accuracy. The test consists of simply determining whether the variable is within its permissible range of values.

The measured compressor face variables (total temperature and total pressure) are monitored for any changes which would be physically impossible under normal operation. The changes associated with changing flight conditions occur rather slowly and are not

interpreted as a failure. There are fluctuations in these variables when the afterburner is lit. Any flight system must allow these changes to pass through the failure detection logic.

The measured engine variables, with the exception of nozzle area, are tested to determine whether they are within their range of permissible values, that is, the maximum and minimum values the corrected variables can assume. This particular test detects only catastrophic failures (hard failures). The nozzle area is tested to ensure that it is properly following the nozzle area command. This test can be made because the digital control calculates a nozzle area from the command and a dynamic model of the nozzle (ref. 5). If the difference between the actual area and the calculated area exceeds a specified value, the nozzle area sensor is assumed to have failed.

Action under Failure

When a sensor failure has been detected, the action taken depends, of course, on the type of failure. One common action under any type of failure is that further learning ceases.

If the command input (power lever angle) is in error, the computer program generates a command which shuts down the engine. Nothing else can be done.

Since the compressor face variables are used to correct the engine measurements, an accurate test of and estimate for engine measurements cannot be made if a compressor face sensor has failed. Therefore, for this type of failure, the engine is shut down by a command from the computer program. Because of the importance of having valid compressor face measurements, these sensors should probably be redundant.

In the case of a nozzle area sensor failure, the invalid measurement is replaced by the calculated value used in the detection of the failure.

For the case of a single failure of one of the four remaining engine sensors, an estimate is made from the three valid measurements and the tables of stored data. For each valid measurement, an estimate is obtained from the appropriate table (for the particular bleed condition and engine dynamic state) relating the two variables by linear interpolation between the stored values. An average of the three estimates is taken, and the resultant value is used by the engine control. In this case and in those for which more than one estimate is available, the estimates are weighted equally. No work was done on examining the effect of unequal weighting. In the case of two failures, the action is similar except this time only two values are averaged to obtain an estimate for each of the two invalid measurements. In the case of three failures, an estimate for each of the three invalid measurements is made from the single remaining valid measurement. In the highly unlikely case of four failures, the computer program commands the engine to shut down.

Bleed Control under Failure

Because the bleeds are controlled by measured variables and the estimates for invalid measurements are a function of the bleed position, it is important to assure that the bleeds operate properly under failure.

The seventh-stage bleed is controlled by the Mach number signal only, which is assumed to be always correct. Therefore, the seventh-stage-bleed condition will always be correct under all allowable failures.

The twelfth-stage bleed is controlled by the low-pressure-compressor discharge static pressure and the compressor face total pressure. If the low-pressure-compressor-discharge-static-pressure sensor should fail, a value is estimated for it by the procedure described previously. If the estimated value is close enough to the actual value, the bleed should operate normally. If the compressor-face-total-pressure sensor should fail, the engine is shut down as previously stated.

Computer Program Outline

A flow chart of the sensor fail-operational digital computer program is presented in figure 7. The numbers on the following outline correspond to the numbers on the flow chart:

(1) The engine measurements are corrected. The three pressures are divided by δ, the ratio of compressor face total pressure to standard sea-level pressure; the high-pressure-rotor speed is divided by $\sqrt{\theta}$, θ being the ratio of the compressor face total temperature to standard sea-level temperature.

(2) The power lever angle is tested. If it is invalid, the engine is shut down.

(3) The compressor face total pressure and total temperature sensors are tested. If either has failed, the engine is shut down.

(4) A test is performed to determine whether sufficient data have been learned. If not, data for the current operating point are learned and the program is exited.

(5) If sufficient data have been learned, the engine measurements are tested.

(6) If there are no sensor failures, data for the current operating point are learned and the program is exited.

(7) If all the engine sensors (not including nozzle area) have failed, the engine is shut down.

(8) Values for the invalid engine measurements are estimated from the valid measurements and the tables of stored data.

RESULTS AND DISCUSSION

Comparison of Measured Engine Variable Relations

The method of estimating values for invalid engine measurements is based upon the assumption that the relations between the corrected measured engine variables remain nearly the same at all flight conditions. In order to determine if this is indeed so, data were collected at the five flight conditions indicated by the circular symbols in figure 2. It would have been preferable to examine the points of extreme compressor face total pressure and temperature indicated in the figure; however, these points were beyond the range of the engine simulation. The selected points are sea-level static; a typical cruise condition, Mach 0.8 at 9.2-kilometer (30 000-ft) altitude; a flight condition at which the compressor face total pressure is high, Mach 1.2 at 3.0-kilometer (10 000-ft) altitude; a flight condition at which the compressor face total temperature is high, Mach 2.2 at 15.2-kilometer (50 000-ft) altitude; and a supersonic flight condition at which the compressor face pressure and temperature are nearly equal to the values for the subsonic cruise condition, Mach 1.2 at 12.2-kilometer (40 000-ft) altitude. The values for the compressor face variables and the correction factors for each flight condition are listed in the following table:

Flight condition			Compressor face total temperature, TT2		Compressor face total pressure, PT2		Temperature correction factor, $\sqrt{\theta} = \sqrt{\frac{TT2}{TSTD}}$	Pressure correction factor, $\delta = \frac{PT2}{PSTD}$
Mach number, M	Altitude, h							
	km	ft	K	^{o}R	N/cm^2	psi		
(a)	(a)	(a)	288	519	10.1	14.7	1	1
.8	9.2	30×10^3	258	465	4.6	6.7	.95	.45
1.2	3.0	10	346	622	16.9	24.5	1.10	1.67
1.2	12.2	40	279	511	4.5	6.6	.99	.45
2.2	15.2	50	426	767	11.2	16.3	1.22	1.11

[a]Sea-level static.

The relations between the measured engine variables were obtained by first clearing the tables of any stored data and then using the self-learning feature of the sensor fail-operational digital computer program at each flight condition. The procedure involved running the simulated engine over the complete range of power lever angle for all possible bleed settings and for both steady-state operation and engine acceleration.

The data obtained in this manner were then compared. Examples of the relations between the measured engine variables are presented in figure 8. The examples show all six possible relations involving the four variables for steady-state operation and for

both bleeds being closed, except the Mach 2.2, 15.2-kilometer (50 000-ft) flight condition, for which the seventh-stage bleed is open. It can be seen from this figure that there is little difference among the data for all the flight conditions, with the exception of sea-level static. The difference between the data at sea-level static and those at the other conditions is explained by the fact that the nozzle is unchoked at the sea-level static condition over most of its range. At the other flight conditions the nozzle is choked over most or all of its range of power lever angle.

The difference in the data for these cases appeared to be significant enough to require the storing of two sets of data: one for the choked nozzle, the other for the unchoked nozzle. The following test was included to determine the nozzle condition: If the ratio of ambient pressure to nozzle total pressure is greater than the critical value (P0/PT7 $>$ 0.542), the nozzle is unchoked. Unchoked nozzle data were collected at sea-level static operation, and choked nozzle data were collected at the Mach 0.8, 9.2-kilometer (30 000-ft) flight condition. The test for the nozzle condition also determines what set of data is to be used in estimating a value for any invalid measurement; but the test of the nozzle condition requires one of the measured engine variables, the nozzle total pressure. If this particular sensor should fail, there would be no way of determining which set of data should be used. An arbitrary decision was made to use the choked nozzle data when the nozzle total pressure sensor was found to have failed.

Figure 9 illustrates the effect twelfth-stage bleed has on the measured engine variable data. This particular example shows the steady-state relation between the corrected high-pressure-rotor speed and the corrected high-pressure-compressor discharge static pressure for the twelfth-stage bleed open and closed. Data are shown for two flight conditions: sea-level static; and Mach 0.8, 9.2-kilometer (30 000-ft) altitude. It can be seen that opening the twelfth-stage bleed has the effect of shifting both curves to the right; that is, the pressure associated with a particular rotor speed is higher with the bleed open. The difference between the two cases appears to be great enough to require storing both sets of data.

Only one flight condition was examined for which the seventh-stage bleed was open: Mach 2.2, 15.2 kilometers (50 000 ft). At this flight condition, a lower limit on engine speed imposed by the control does not allow much variation in the measured engine variables. Over this small range, there appears to be no difference between the data collected with the seventh-stage bleed open and with it closed. This is illustrated in figure 10 in which the steady-state relation between the corrected high-pressure-rotor speed and the corrected high-pressure-compressor discharge static pressure is presented. It seems that separate data for the two cases need not be collected.

Separate data were also collected for steady-state operation and for operation when the fuel flow was limited by the acceleration schedule in the control. An example of the data for these two cases is shown in figure 11. It shows the relation between high-pressure-rotor speed and high-pressure-compressor discharge static pressure for both

steady-state operation and acceleration at two flight conditions: sea-level static; and Mach 0.8, 9.2-kilometer (30 000-ft) altitude. The difference between the data sets is small at the altitude condition. At sea-level static operation, the difference between the two sets of data is somewhat greater.

The approach taken in this study was to collect data for all possible engine geometries and dynamic conditions, as well as for both nozzle conditions, to obtain the best possible fail-operational control system. After this, the control system was tested using less complete data to determine just how much information is necessary to obtain acceptable results.

Limits on Estimated Variables

When a measured engine variable sensor has failed and the measured value is replaced with an estimate obtained from the other measurements, there is a possibility that the estimated value may change the operation of the engine and hence the measurements that are used to estimate a value for the invalid measurement. This could result in an unstable situation in some cases. Limits had to be put on the estimated values of two measured engine variables at the extreme values of power lever angle. A lower limit had to be placed on the estimated value of high-pressure-compressor discharge static pressure. When this variable is estimated low at a low value of power lever angle, the fuel flow, which is controlled by this pressure and the high-pressure-rotor speed, decreases. This causes a reduction in the measured variables used to estimate compressor pressure and hence a reduction in the estimated value of this variable. The process continues until the fuel flow stops altogether. This problem was encountered only at near-idle values of power lever angle and was solved by placing a lower limit on the estimated value of high-pressure-compressor discharge static pressure equal to the value that it normally would have at idle for the particular nozzle condition.

It was also necessary to impose this lower limit on high-pressure-compressor discharge static pressure when the high-pressure-rotor-speed sensor failed at low values of power lever angle. If the speed is estimated high, the fuel flow decreases. This reduces the actual speed and also the high-pressure-compressor discharge static pressure, which in turn tends to reduce fuel flow. The difference between the requested speed and the estimate of the actual speed tends to increase the fuel flow. But its effect is not sufficient to offset the reduction caused by the decreased value of high-pressure-compressor discharge static pressure. Consequently, the fuel flow continues to decrease until the engine stops running.

An upper limit on the estimated value of nozzle total pressure was necessary during afterburning operation, that is, when the power lever angle was above 69°. As mentioned previously, this pressure determines the nozzle area and the afterburner-zone

fuel flows. If it is estimated high, the nozzle opens more than it should, decreasing the actual value of the nozzle total pressure. This tends to increase the low-pressure-rotor speed and the low-pressure-compressor discharge static pressure, which tends to further increase estimated nozzle total pressure. This process continues, causing abnormal nozzle and zone fuel-flow operation. The difficulty was corrected by limiting nozzle total pressure to the value that it has just before afterburning begins. This essentially eliminated nozzle total pressure as a control variable for the nozzle and zone fuel flows. The control function was fulfilled by the other variables: high-pressure-compressor discharge pressure and high-pressure-rotor speed.

There might be a problem with this latter limit as the flight condition is changed while the engine remains in afterburning operation. This could be solved by changing the limit on nozzle pressure when the values of compressor face total temperature and pressure change by some specified amount, indicating a large change in flight condition.

The nozzle pressure measurement is also used to detect afterburner light-off and blowout. If this particular measurement is being estimated from other engine measurements, errors in the estimate cause no serious operational limit violations during light-off. However, in the case of a blowout, the error in the estimated nozzle total pressure causes serious operational limit violations. Therefore, provision would have to be made to detect blowouts in some other manner.

Engine Performance

The unchoked nozzle data obtained at sea-level static condition and the choked nozzle data obtained at the Mach 0.8, 9.2-kilometer (30 000-ft) flight condition were stored in the computer. Learning was then halted so that no additional data would be averaged with the original data. The sensor fail-operational control system was then tested at each of the five selected flight conditions. At each condition, all combinations of the four engine sensors (not including nozzle area) were failed, and the simulated engine was subjected to throttle variations from idle to military power (power lever angle from 15° to 69°) and from idle to full afterburning (power lever angle from 15° to 120°). Throttle variations were made both slowly, to simulate a series of steady-state operating points, and rapidly, to determine performance for throttle slams and chops.

The effectiveness of the sensor fail-operational control system was judged by the following two criteria: First, it was necessary that none of the engine operating limits be exceeded: the surge margin of either of the two compressors or the fan may not be reduced; the turbine-inlet-temperature limit may not be exceeded; and the high-pressure-rotor-speed limit may not be exceeded. Second, it was desirable that the performance of the engine not be degraded; that is, that nearly the same thrust be obtained at a particular power lever angle and nearly the same thrust response result

from a change in power lever angle.

The significant results were these: For nonafterburning operation (power lever angle less than 69°), the simulated engine could be acceptably controlled with as many as three of the four engine sensors failed. One of the four variables, nozzle total pressure, does not affect operation when there is no afterburning; so its failure had no effect. Another variable, the low-pressure-compressor discharge static pressure, affects the twelfth-stage-bleed operation only. Results indicate that an acceptable value could be estimated for this variable from only one valid measurement. Acceptable values for the other two variables could also be obtained from only one valid measurement. For operation in the afterburning range (power lever angle from 69° to 120°), the engine could be acceptably controlled with no more than a single sensor failure, and then only if a modest, power-lever-angle rate limit is imposed (approx. 3 deg/sec). The low-pressure-compressor-discharge-static-pressure sensor could not be failed along with any of the other sensors even though it does not affect afterburning operation. Apparently, estimates based on this variable are needed to construct values for any invalid measurement.

It is suspected that the limitation on failures in the afterburning range and the need for a power-lever-angle rate limit arise primarily from the use of an integrator loop (which eliminates steady-state error) in the afterburner control. This type of control is more sensitive to any difference between an estimated value for a variable and the true value it replaces.

Even with only a single failure of one of the variables affecting afterburning operation, the fifth-zone afterburner fuel flow in some cases was somewhat different from normal. The differences were not considered to be great enough to cause any difficulty.

Acceptable control was defined earlier as not violating any of the engine operating limits and providing nearly the same thrust response. In order to illustrate a typical comparison between engine performance under sensor fail-operational control and normal performance, a series of figures is presented for one particular single failure, that of a high-pressure-rotor-speed sensor. The assumed flight condition is Mach 1.2 and 3.0-kilometer (10 000-ft) altitude. This flight condition was selected because the difference between the pressure correction factor at this condition and that at which the data were learned is greater than that for any other flight conditions examined. Figure 12 compares the loci of operating points for failed and normal performance on both the low-pressure- and high-pressure-compressor maps for steady-state operation and for a throttle slam from idle to full afterburning. Figure 13 compares high-pressure-rotor speed for failed and normal performance. For the failed case, both the actual speed and the estimated speed used by the control are presented. Figure 14 compares turbine inlet temperature for the two cases. The thrust obtained with a high-pressure-rotor-speed sensor failure is compared with normal thrust in figure 15. These figures indicate that the simulated engine performs fairly normally under sensor fail-operational

control with the high-pressure-rotor-speed sensor failure.

A similar set of comparisons for a double failure is presented in figures 16 to 19. In this case, the two sensor failures are high-pressure-rotor speed and high-pressure-compressor discharge static pressure. The flight condition is again Mach 1.2 and 3.0-kilometer (10 000-ft) altitude. However, power lever angle is varied only from idle to military power. Failure of these two sensors means that main fuel flow must be controlled with only estimated values for the necessary variables. Again, these figures indicate that the simulated engine under sensor fail-operational control performs very nearly as it does normally.

Operation with Reduced Data Storage

Previous comparisons of the stored data for any particular flight condition reveal small differences between some of the curves. For example, the data for seventh-stage bleed open do not differ much from that for it closed (fig. 10). The sensor fail-operational program was again tested at the flight condition for which the seventh-stage bleed is open: Mach 2.2 and 15.2-kilometer (50 000-ft) altitude. This time, however, the data obtained when the seventh-stage bleed was closed were used. There appeared to be no difference in performance. It is believed that data need not be collected for seventh-stage bleed open. This reduces the data storage requirement and simplifies the collecting of data.

Operation of the sensor fail-operational control system with only one set of twelfth-stage-bleed data, either for the bleed open or closed, did not produce satisfactory performance. Apparently, the differences between the relations in the two cases are sufficiently great to require both sets of data to be stored.

The data curves obtained during acceleration compare closely with the curves obtained for steady-state operation (fig. 11). Based on this observation the sensor fail-operational control system was tested by using the steady-state data to estimate values during acceleration. The performance of the simulated engine for this test was essentially the same as that obtained when the acceleration data were used. An example of this result is presented in figures 20 to 23. The case shown is for a throttle slam from idle to full afterburning with a high-pressure-rotor-speed sensor failure. The flight condition is again Mach 1.2 and 3.0-kilometer (10 000-ft) altitude. These figures compare the performance obtained with steady-state data and that obtained with acceleration data. Figure 20 compares the loci of operating points on both the low-pressure- and high-pressure-compressor maps; figure 21 compares the high-pressure-rotor speeds; figure 22, the turbine inlet temperatures; and figure 23, the thrust responses. Based on results of this type, it appears that separate acceleration data need not be collected.

Even though there is a large difference between the data collected when the nozzle

is choked and when it is unchoked, the sensor fail-operational control system was tested using the unchoked data only (data collected at sea-level static operation). Surprisingly, for the most part the results were the same as those obtained with the two separate sets of data. In some cases, however, there was a slight reduction in high-pressure-compressor surge margin. It appears that it might be possible to collect data at sea-level static operation only. This would greatly simplify the collection of data if it is to be learned. The lower limit on high-pressure-compressor discharge static pressure had to be modified for this test. At any of the flight conditions other than sea-level static (i.e., when the nozzle is choked), the lower limit on this pressure was set equal to the value it normally would have at idle at the respective flight conditions. This value would either have to be learned or predetermined.

Computer Requirements

The sensor fail-operational digital computer program (exclusive of the stored data) requires about 2000 words of core storage. The complete set of stored engine data requires 4600 words of core storage. This latter requirement can be cut in half if acceleration data are not stored and further reduced by 1/3 if data for open seventh-stage bleed are not stored. Also, the number could be reduced by using less than the 64 words for each data curve. Even with the 4600 words of data, the total storage requirement of the sensor fail-operational program is only 6600 words. This requirement, added to the 5000-word requirement for the BOM control, comes to 11 600. With a 16 000-word-storage computer, over 4000 words would be available for other tasks.

The computation time required by the sensor fail-operational digital computer program depends upon a number of factors. During learning (when no variable estimation is being done), the computation time depends upon the number of data points that are being learned during that particular cycle. The maximum computation time observed during learning was about 13 milliseconds. During engine variable estimation (when no additional learning takes place), the computation time depends upon the number of measurements that must be estimated. The time is not directly proportional to the number of failures, however, because the number of table lookups (which require the most time) is not proportional to the number of failures. Estimation of a single variable requires about 3 milliseconds; both a double and a triple failure require about 4 milliseconds. As stated previously, a sampling interval of 25 milliseconds was selected for this study. The maximum time required by the sensor fail-operational digital computer program added to the 3 milliseconds required by the digital BOM control comes to 16 milliseconds. About 9 milliseconds of computation time would be available for other tasks. It is felt that with more efficient programming, computation time could be reduced considerably.

CONCLUSIONS

The study indicates that a sensor fail-operational control system can be used to provide acceptable control of a two-spool turbofan engine over a wide range of flight conditions with as many as three of the four engine sensors failed for nonafterburning engine operation. For afterburning operation, the sensor fail-operational system provides acceptable control for only a single engine sensor failure. In this case, it is necessary that a slight limit be imposed upon engine acceleration. Because such an extreme range of compressor face conditions was investigated, the results obtained are applicable over a wide range of flight conditions. Further testing is required to ensure that results are applicable over the entire engine operating envelope.

The sensor fail-operational control system was evaluated on a real-time, nonlinear, hybrid-computer simulation of a turbofan engine. The results of this study should be verified by using the system to control an actual engine.

The engine variables were tested for catastrophic sensor failure only. The failure-detection part of the system could be expanded so that other types of failures can be handled. This is an area in which further work could be done.

The Mach number measurement, which is received from the inlet control, was assumed to be always correct. In an integrated inlet and engine control system, it might be possible to handle a failure of this variable.

Finally, it should be noted that this particular sensor fail-operational control system was designed to be "added on" to a digital representation of the basic bill-of-materials hydromechanical control system. Fail-operational requirements could have an effect upon the design of a completely new control system. Such a system may not have some of the limitations reported herein.

Lewis Research Center,
National Aeronautics and Space Administration,
Cleveland, Ohio, July 30, 1975,
505-05.

APPENDIX - SYMBOLS

AJ	nozzle area, m^2 (ft^2)
AJC	commanded nozzle area, m^2 (ft^2)
BL7	seventh-stage bleed
BL12	twelfth-stage bleed
F	net thrust, N (lbf)
h	altitude, km (ft)
M	Mach number
N2	high-pressure-rotor speed, rpm
$N2/\sqrt{\theta}$	corrected high-pressure-rotor speed, rpm
PLA	power lever angle, deg
PSTD	standard-day, sea-level pressure, 10.1 N/cm^2 (14.7 psi)
PS3	low-pressure-compressor discharge static pressure, N/cm^2 (psi)
PS3/δ	corrected low-pressure-compressor discharge static pressure, N/cm^2 (psi)
PS4	high-pressure-compressor discharge (combustor) static pressure, N/cm^2 (psi)
PS4/δ	corrected high-pressure-compressor discharge (combustor) static pressure, N/cm^2 (psi)
PT2	compressor face total pressure, N/cm^2 (psi)
PT7	nozzle total pressure, N/cm^2 (psi)
PT7/δ	corrected nozzle total pressure, N/cm^2 (psi)
P0	ambient pressure, N/cm^2 (psi)
TSTD	standard-day, sea-level temperature, 288 K (519° R)
TT2	compressor face total temperature, K ($^{\circ}$R)
T5	turbine inlet temperature, K ($^{\circ}$R)
t	time, sec
WF	main fuel flow, kg/sec (lbm/sec)
WFZn	zone n afterburner fuel flow (n = 1, ..., 5), kg/sec (lbm/sec)
δ	ratio of compressor face total pressure to standard-day sea-level pressure, PT2/PSTD

θ ratio of compressor face total temperature to standard-day sea-level temperature, TT2/TSTD

Engine station numbers (fig. 1):

2 compressor face

3 low-pressure-compressor discharge

4 high-pressure-compressor discharge

5 turbine inlet

7 nozzle

REFERENCES

1. Beard, Richard V.: Failure Accommodation in Linear Systems Through Self-Reorganization. (MVT-71-1, Mass. Institute of Tech.; Grant NGL-22-009-025), NASA CR-118314, 1971.

2. Montgomery, R. C.; and Caglayan, A. K.: A Self-Reorganizing Digital Flight Control System for Aircraft. AIAA Paper 74-21, Feb. 1974.

3. Ellis, Stanley H.: Self-Correcting Control for a Turbofan Engine. PWA-FR-6778, Pratt & Whitney Aircraft Florida Research and Development Center, 1975.

4. Wallhagen, Robert E.; and Arpasi, Dale J.: Self-Teaching Digital-Computer Program for Fail-Operational Control of a Turbojet Engine in a Sea-Level Test Stand. NASA TM X-3043, 1974.

5. Cwynar, David S.; and Batterton, Peter G.: Digital Implementation of the TF30-P-3 Turbofan Engine Control. NASA TM X-3105, 1975.

6. Szuch, John P.; and Bruton, William M.: Real-Time Simulation of the TF30-P-3 Turbofan Engine Using a Hybrid Computer. NASA TM X-3106, 1974.

7. Arpasi, Dale J.; Cwynar, David S.; and Wallhagen, Robert E.: Sea-Level Evaluation of Digitally Implemented Turbojet Engine Control Functions. NASA TN D-6936, 1972.

8. Arpasi, Dale J.; Zeller, John R.; and Batterton, Peter G.: A General Purpose Digital System for On-Line Control of Airbreathing Propulsion Systems. NASA TM X-2168, 1971.

9. Sanders, Newell D.: Performance Parameters for Jet-Propulsion Engines. NACA TN 1106, 1946.

TABLE I. - VARIABLES USED FOR CONTROL OF TF30-P-3 ENGINE

Variable	Symbol
Command input: power lever angle	PLA
Flight condition:	
Mach number	M
Ambient pressure	P0
Measured compressor face:	
Total temperature	TT2
Total pressure	PT2
Measured engine:	
High-pressure-rotor speed	N2
High-pressure-compressor discharge static pressure	PS4
Low-pressure-compressor discharge static pressure	PS3
Nozzle total pressure	PT7
Nozzle area	AJ
Manipulated:	
Main fuel flow	WF
Seventh-stage bleed	BL7
Twelfth-stage bleed	BL12
Nozzle area	AJC
Afterburner fuel flow:	
Zone 1	WFZ1
Zone 2	WFZ2
Zone 3	WFZ3
Zone 4	WFZ4
Zone 5	WFZ5
Controlled: net thrust	F

TABLE II. - DIGITAL SYSTEM CAPABILITIES

Digital computer	
Magnetic core memory size, words	16 384
Word length, bits plus parity	16
Memory cycle time, nsec	750
Add time, μsec	1.5
Subtract time, μsec	1.5
Multiply time, μsec	4.5
Divide time, μsec	8.25
Load time, μsec	1.5
Store time, μsec	1.5
Indirect addressing	Infinite
Indexing	Total memory
Priority interrupts	28 Separate levels
Index registers:	
Independent	1
In conjunction with lower accumulator	1
Physical size, in.:	
Width	24
Height	62
Depth	30
Interval timers	
Complement	2
Accuracy, clock pulses	±1
Clock rates, kHz	572, 286, 160, 143, 80, 71.5, 40, 35, 75, 20, 10
Counter	16-Bit binary
Output	Priority interrupt to computer
Analog acquisition unit	
Overall sample rate (maximum), kHz	20
Resolution of digital data, bits	12 (plus sign)
Output code	Two's complement
Number of channels	64
Input range, V full scale	±10
Input impedance, MΩ (shunted by 10 pF)	10
Maximum source resistance, Ω	1000
Conversion time, μsec	38
Input setting time, μsec	9
Sample-and-hold aperture time, nsec	500
Safe input voltages, V	±20 sustained ±100 for less than 100 μsec
Total error with calibration, percent	0.073

TABLE II. - Concluded.

Frequency acquisition unit	
Number of channels	10
Nature of input	Continuously varying or pulsatile
Resolution of digital data, bits	12
Switch selectable clock rates, kHz	20, 80, 100, 400, external
Overall accuracy, bits	±1
Update rate	Once per cycle of input frequency
Maximum input frequency, kHz	1
Input amplitude range	100 mV to 30 V peak to peak
Analog output unit	
Total number of digital-to-analog conversion channels	26
Resolution (10 channels), bits	12 (plus sign)
Resolution (16 channels), bits	11 (plus sign)
Output voltage range, V full scale	±10
Output current (maximum), mA	10
Output impedance, Ω	<1
Accuracy (12 bit), percent of full scale	±0.1
Accuracy (13 bit), percent of full scale	±0.05
Slew rate, V/μsec	1
Settling time for 10-V step to within 0.05 percent of final value, μsec	20
Logical output unit	
Number of electronic switch outputs	32
Number of contact closure outputs	32
Maximum voltage, V	30
Maximum current, mA	100
Priority interrupt processor	
Number of channels	10
Input impedance, kΩ	47
Input voltage range, V	±10
Comparator switching	Trigger on rise or fall
Comparator hysteresis	Adjustable from 35 mV to 650 mV
Comparator output, V	+7
Monostable multivibrator:	
Pulse width, μsec	.3
Pulse height, V	+7

TABLE III. - TABLES OF STORED, MEASURED ENGINE VARIABLES

Table	Data	Units	Independent variable			
			Range		Increment	
			N/cm^2	psi	N/cm^2	psi
1	$N2/\sqrt{\theta}$ against PT7/δ	rpm, N/cm^2 (psi)	10.3 - 29.0	15 - 42	0.34	0.50
2	$N2\sqrt{\theta}$ against PS4/δ	rpm, N/cm^2 (psi)	20.7 - 207	30 - 300	3.4	5.0
3	$N2\sqrt{\theta}$ against PS3/δ	rpm, N/cm^2 (psi)	0 - 74.5	0 - 108	1.4	2.0
4	PS4/δ against PT7/δ	N/cm^2 (psi)	10.3 - 29.0	15 - 42	.34	.50
5	PS3/δ against PT7/δ	N/cm^2 (psi)	10.3 - 29.0	15 - 42	.34	.50
6	PS3/δ against PS4/δ	N/cm^2 (psi)	20.7 - 207	30 - 300	3.4	5.0

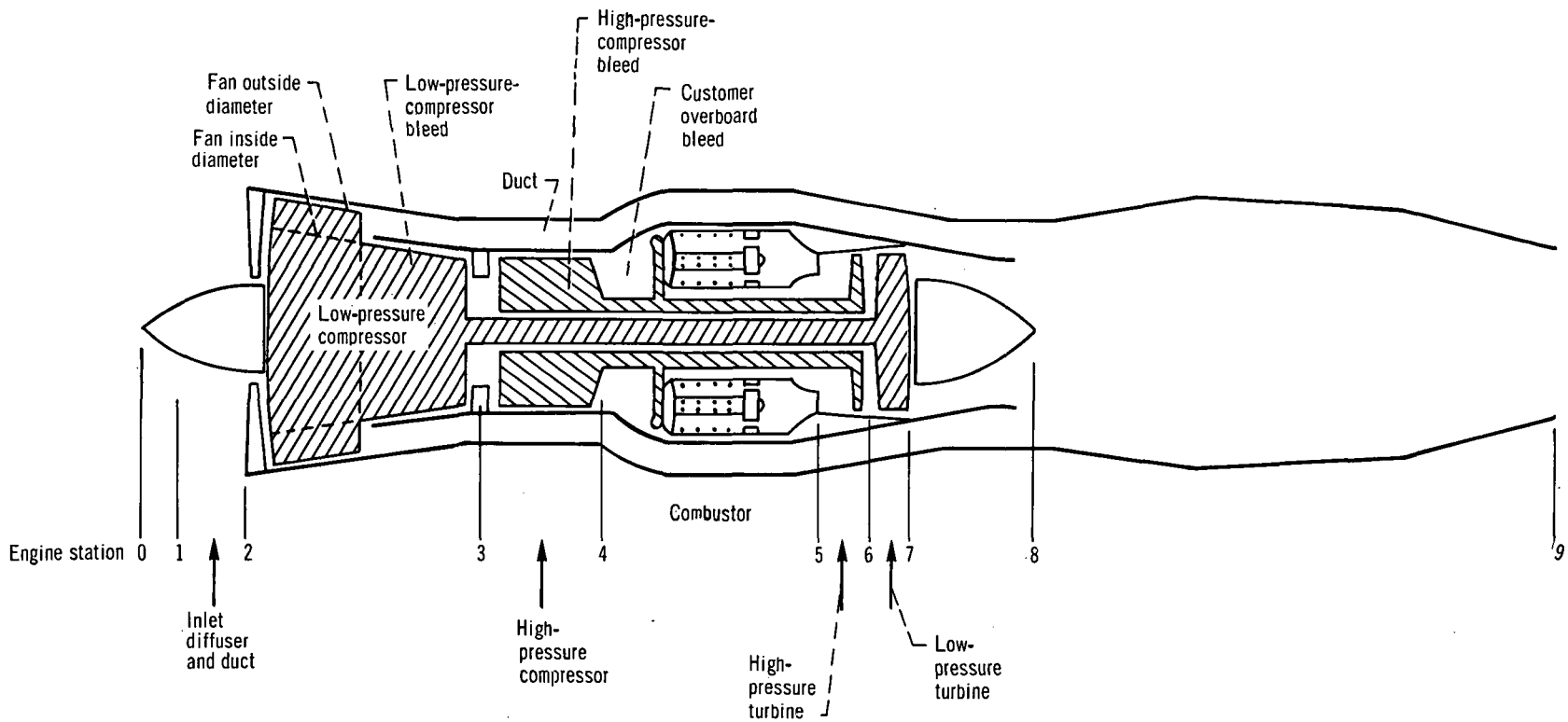

Figure 1. - Schematic representation of TF30-P-3 afterburning turbofan engine with station designations.

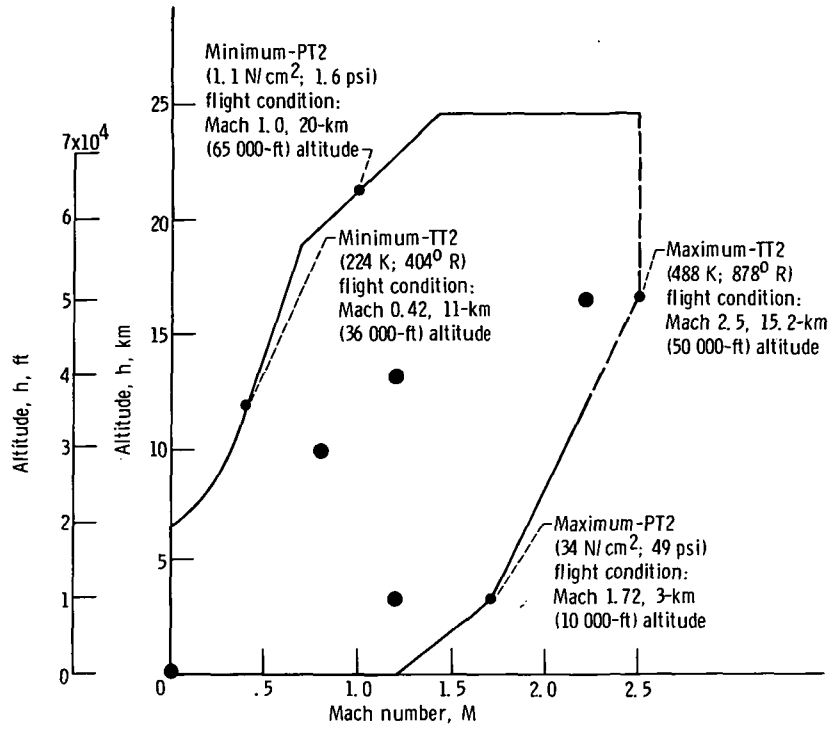

Figure 2. - Engine operating limits for TF30-P-3 engine.

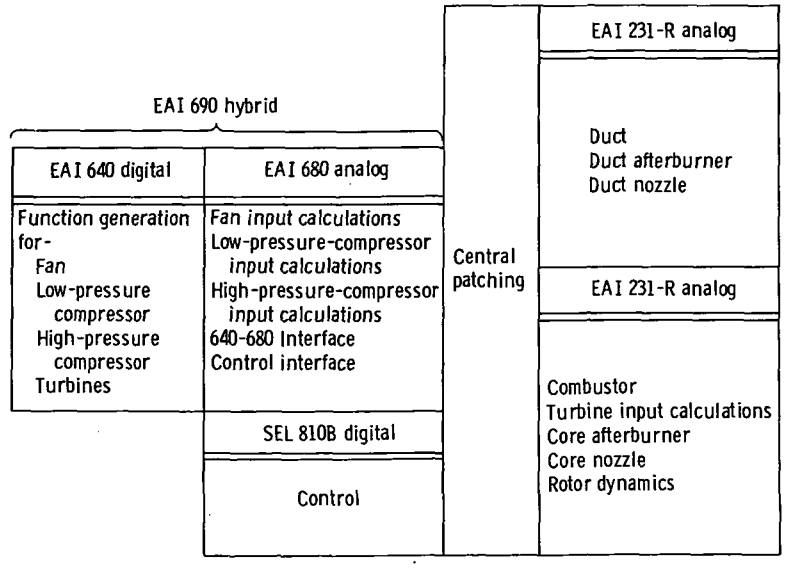

Figure 3. - Split of TF30-P-3 simulation computational load.

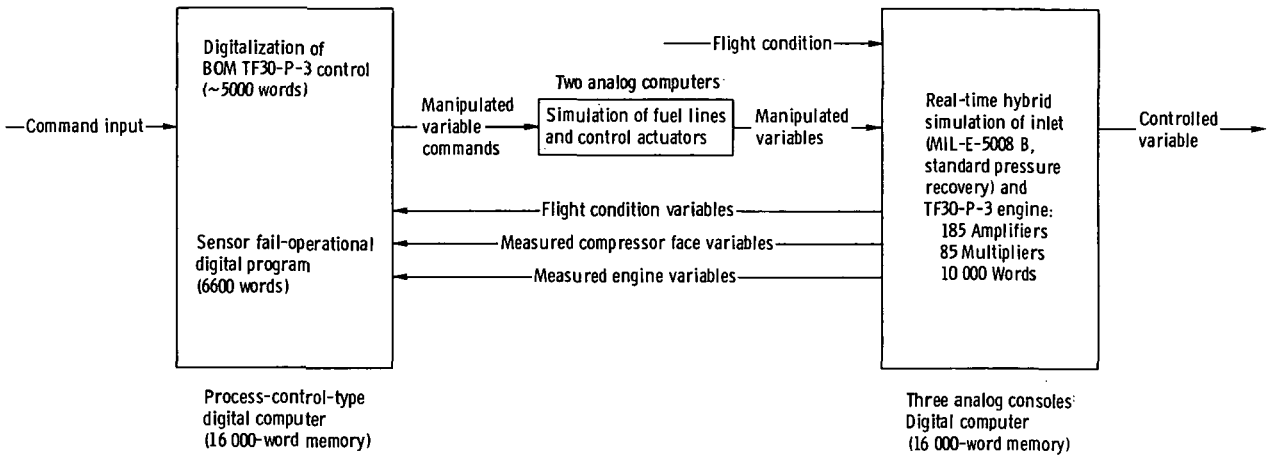

Figure 4. - System used in evaluating sensor fail-operational system.

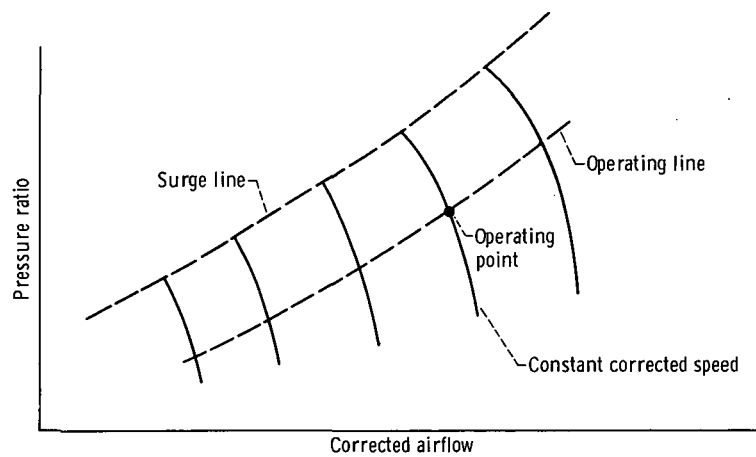

Figure 5. - Schematic representation of a corrected compressor map.

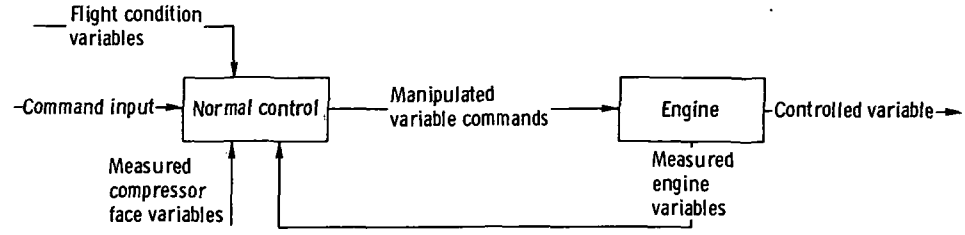

(a) Conventional engine control system.

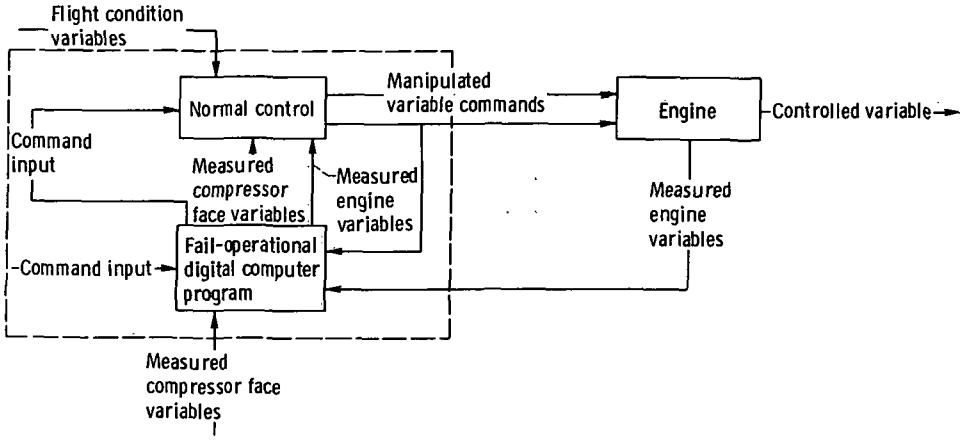

(b) Sensor fail-operational control system.

Figure 6. - Comparison of a conventional engine control system with a sensor fail-operational control system.

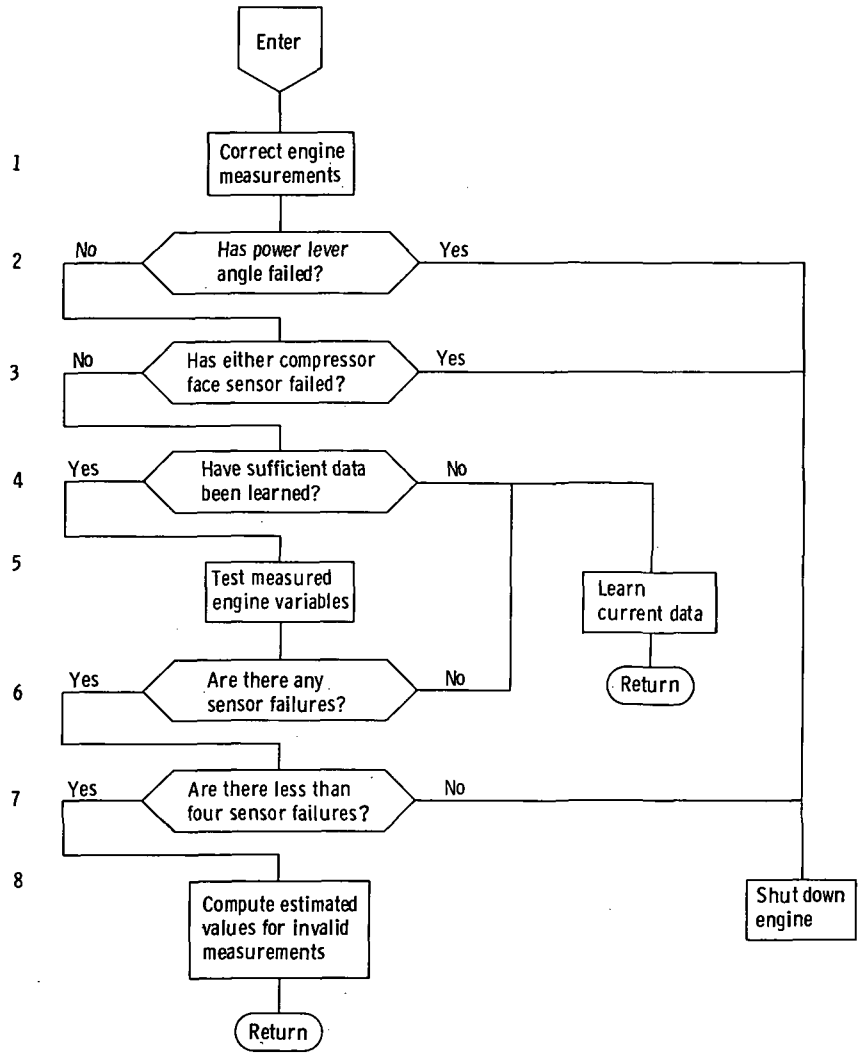

Figure 7. - Flow chart of TF30-P-3 sensor fail-operational digital computer program.

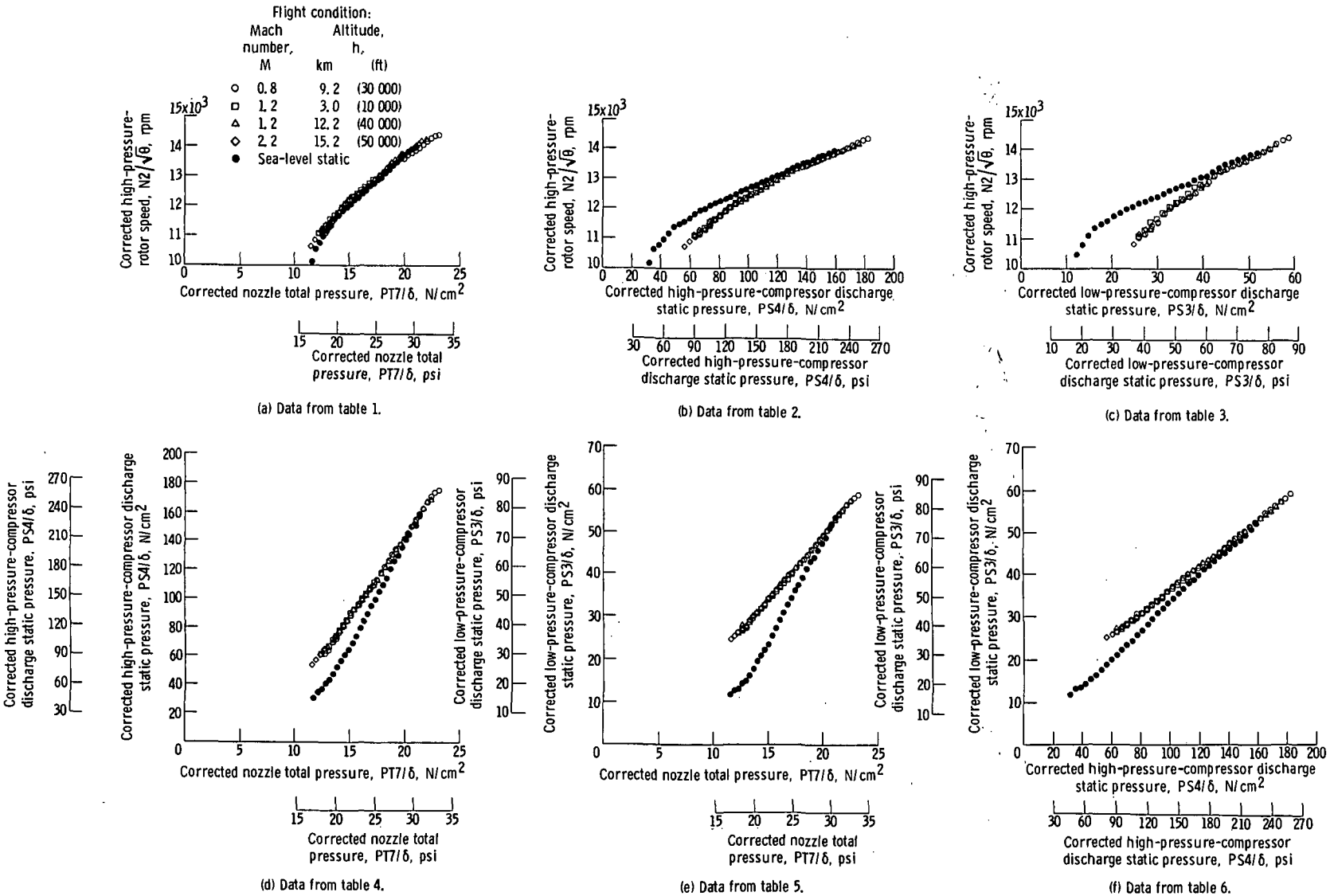

(a) Data from table 1.

(b) Data from table 2.

(c) Data from table 3.

(d) Data from table 4.

(e) Data from table 5.

(f) Data from table 6.

Figure 8. - Comparison of measured engine variable data at five flight conditions. Steady-state operation; twelfth-stage bleed closed; seventh-stage bleed closed for all cases except for the Mach 2.2, 15.2-km (50 000-ft) flight condition.

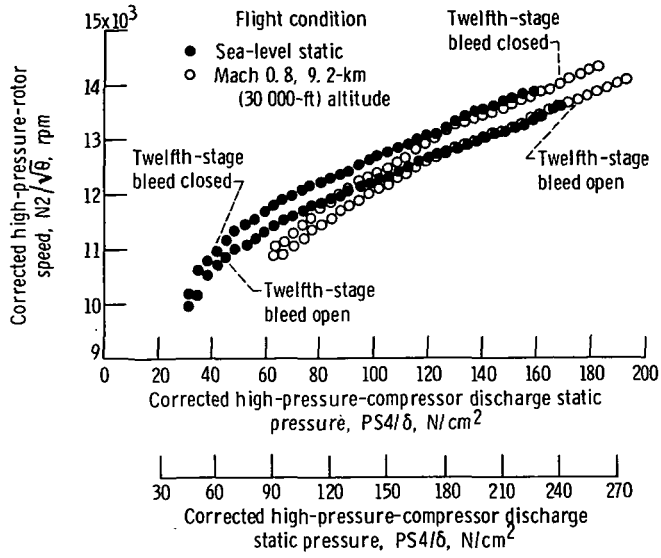

Figure 9. - Effect of twelfth-stage-bleed condition on measured engine variable data for two flight conditions. Steady-state operation; seventh-stage bleed closed. (Data from table 2.)

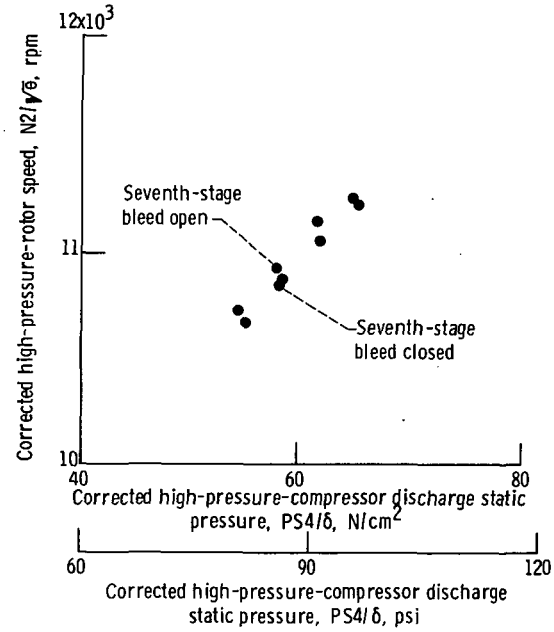

Figure 10. - Effect of seventh-stage-bleed condition on measured engine variable data at Mach 2.2, 15.2-km (50 000-ft) flight condition. Steady-state operation; twelfth-stage bleed closed. (Data from table 2).

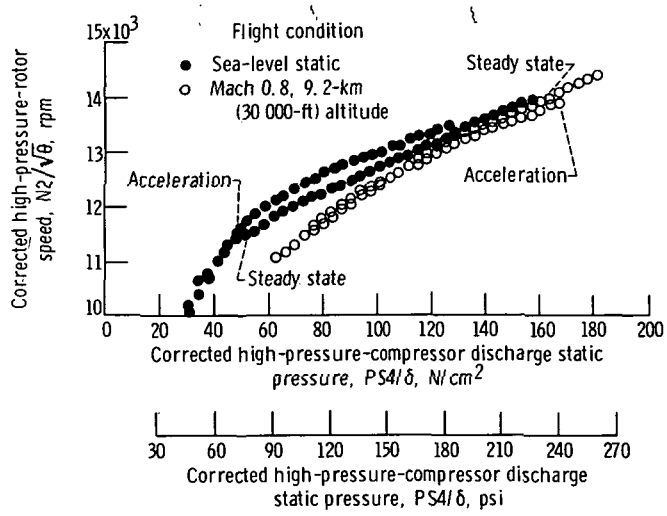

Figure 11. - Comparison of steady-state data with data obtained during engine acceleration for two flight conditions. Both twelfth-stage and seventh-stage bleeds closed. (Data from table 2.)

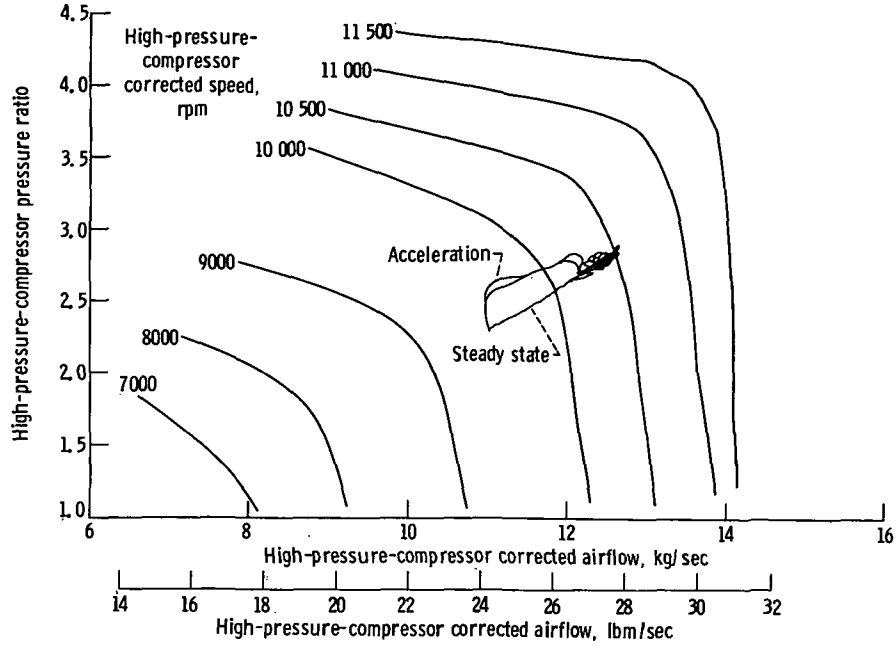

(a) High-pressure compressor.

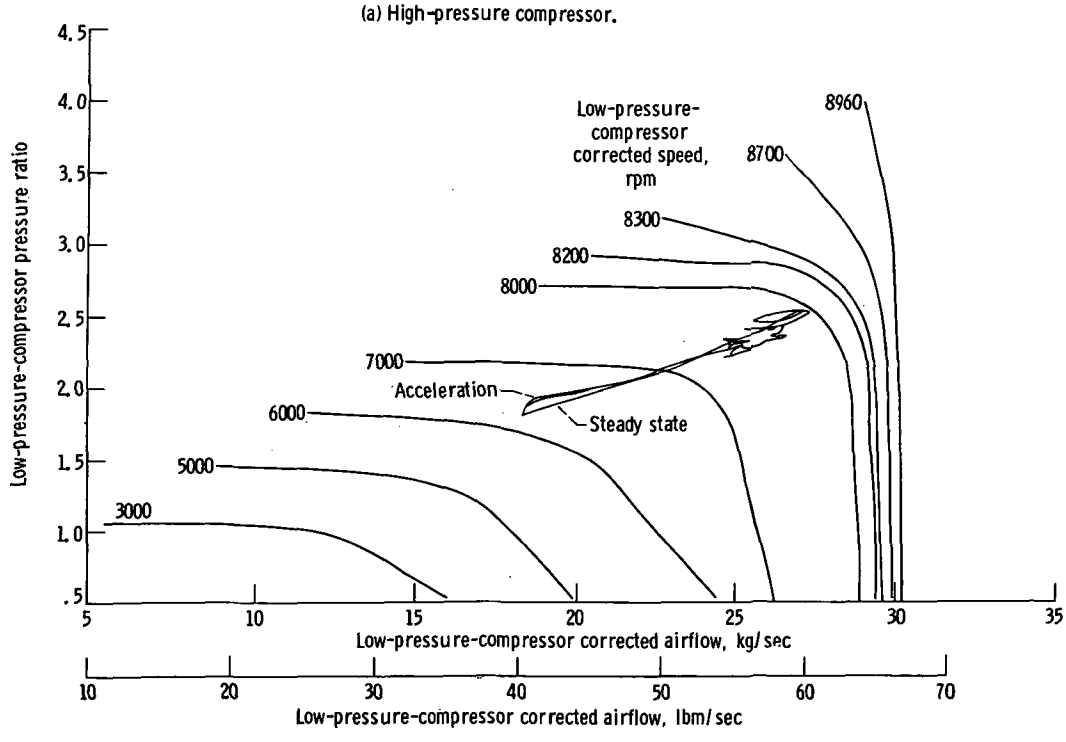

(b) Low-pressure compressor.

Figure 12. - Compressor operating lines for normal operation and for a high-pressure-rotor-speed sensor failure. Flight condition, Mach 1.2 and 3.0-km (10 000-ft) altitude; data obtained at Mach 0.8 and 9.2-km (30 000-ft) altitude.

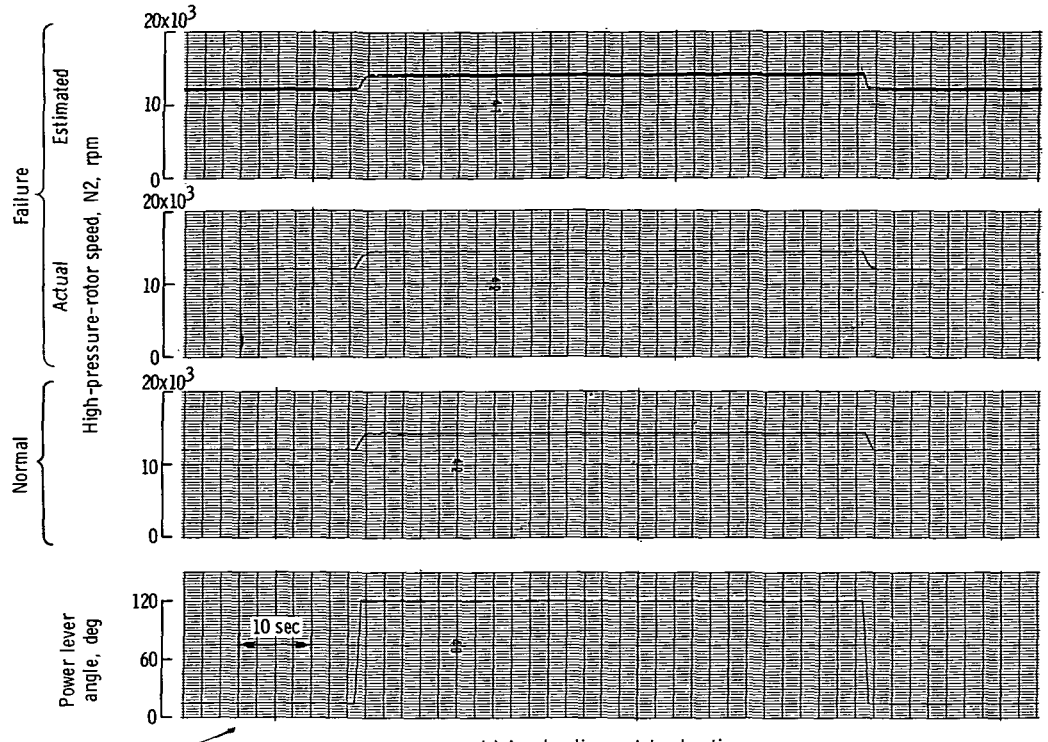

(a) Acceleration and deceleration.

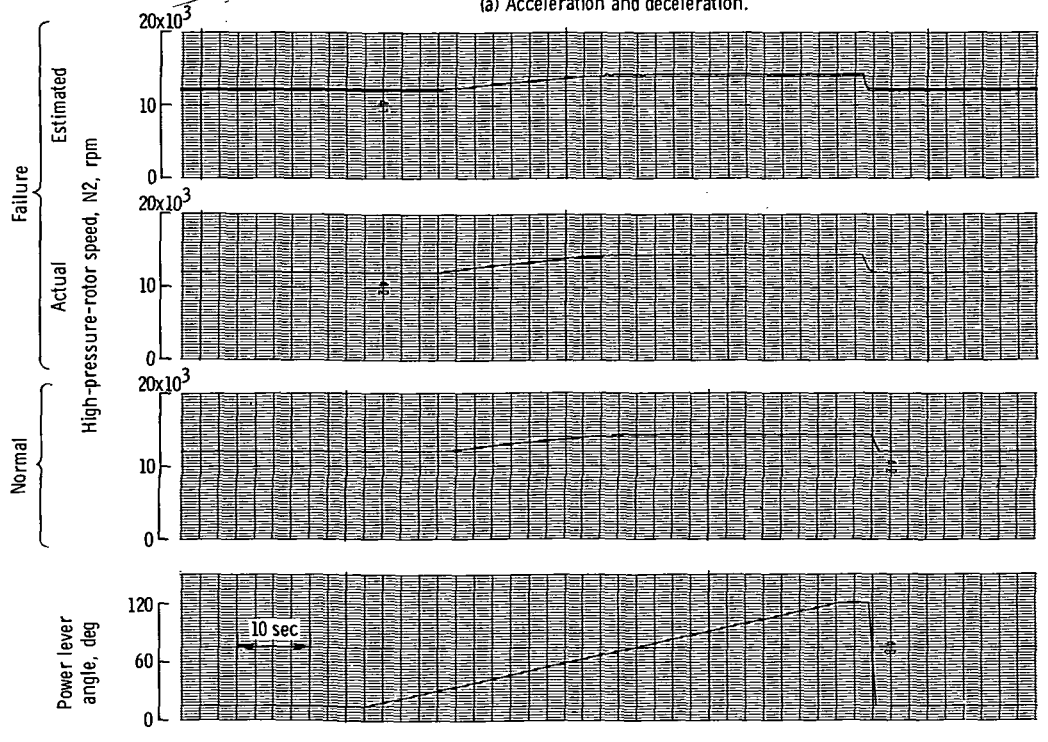

(b) Steady state.

Figure 13. - High-pressure-rotor speed for normal operation and for a high-pressure-rotor-speed sensor failure. Flight condition, Mach 1.2 and 3.0-km (10 000-ft) altitude; data obtained at Mach 0.8 and 9.2-km (30 000-ft) altitude.

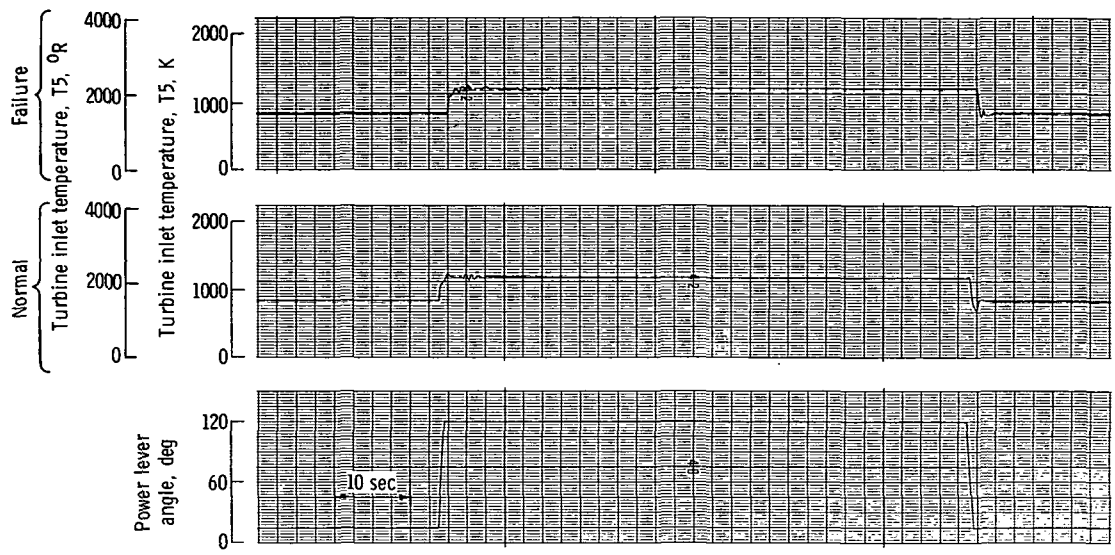

(a) Acceleration and deceleration.

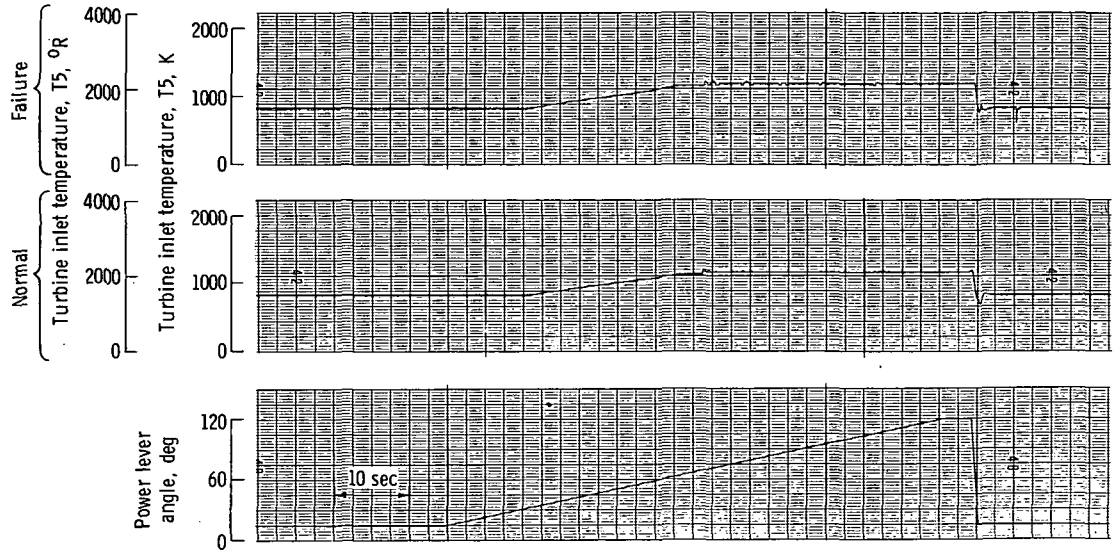

(b) Steady state.

Figure 14. - Turbine inlet temperature for normal operation and for a high-pressure-rotor-speed sensor failure. Flight condition, Mach 1.2 and 3.0-km (10 000-ft) altitude; data obtained at Mach 0.8 and 9.2-km (30 000-ft) altitude.

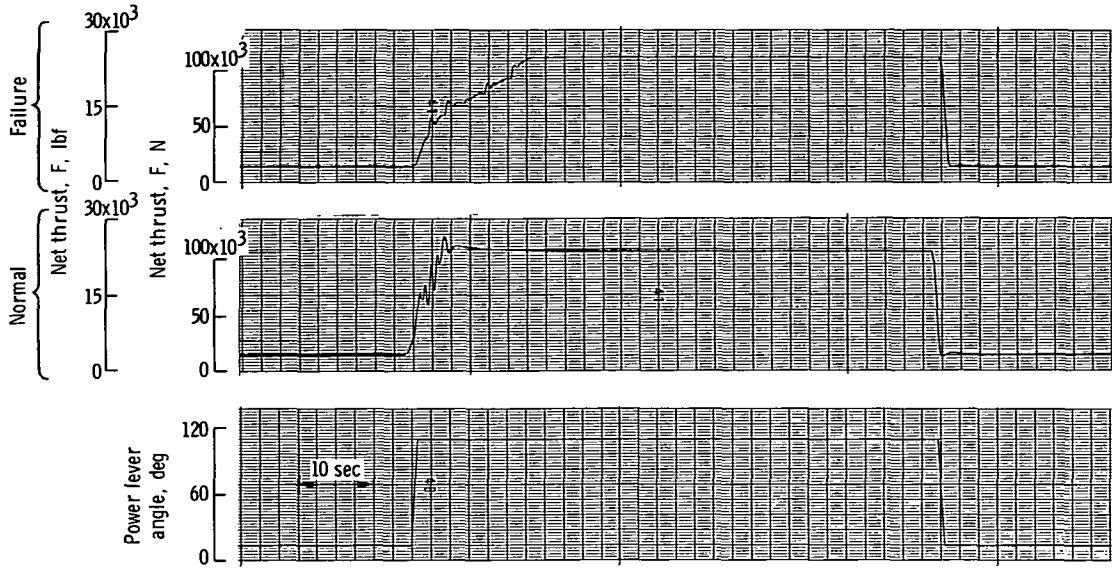

(a) Acceleration and deceleration.

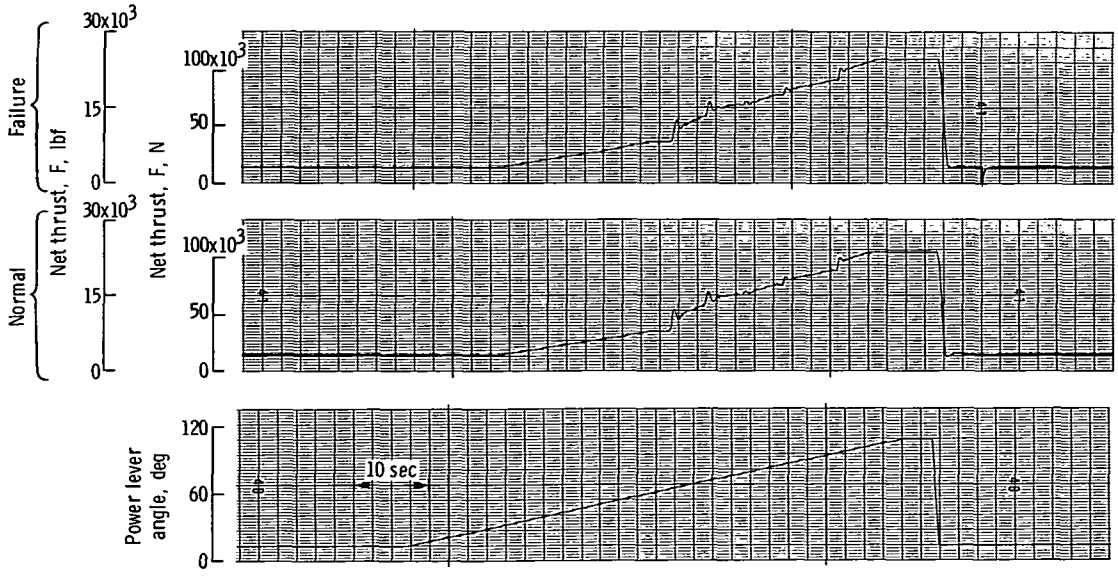

(b) Steady state.

Figure 15. - Net thrust for normal operation and for a high-pressure-rotor-speed sensor failure. Flight condition, Mach 1.2 and 3.0-km (10 000-ft) altitude; data obtained at Mach 0.8 and 9.2-km (30 000-ft) altitude.

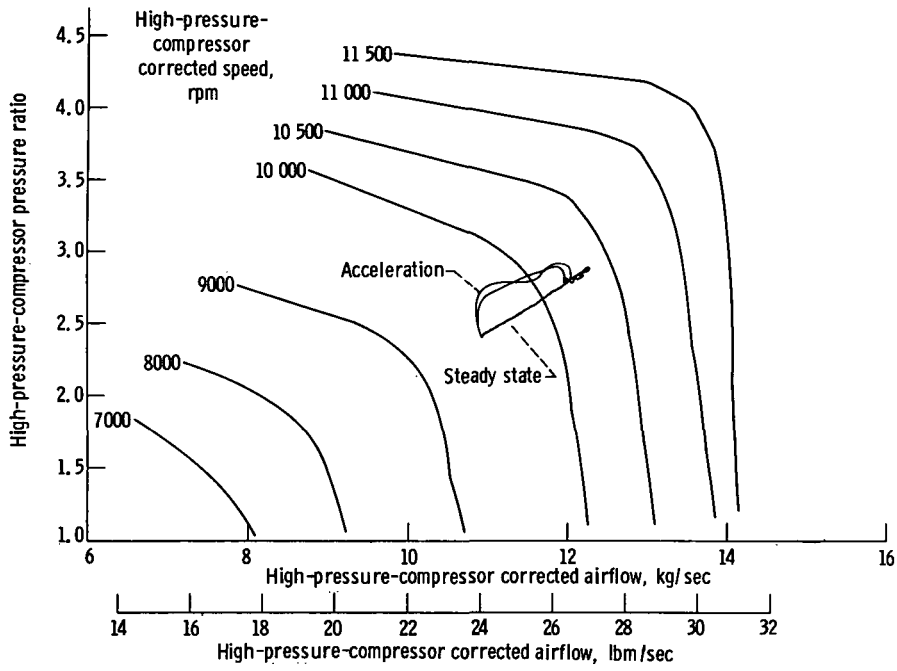

(a) High-pressure compressor.

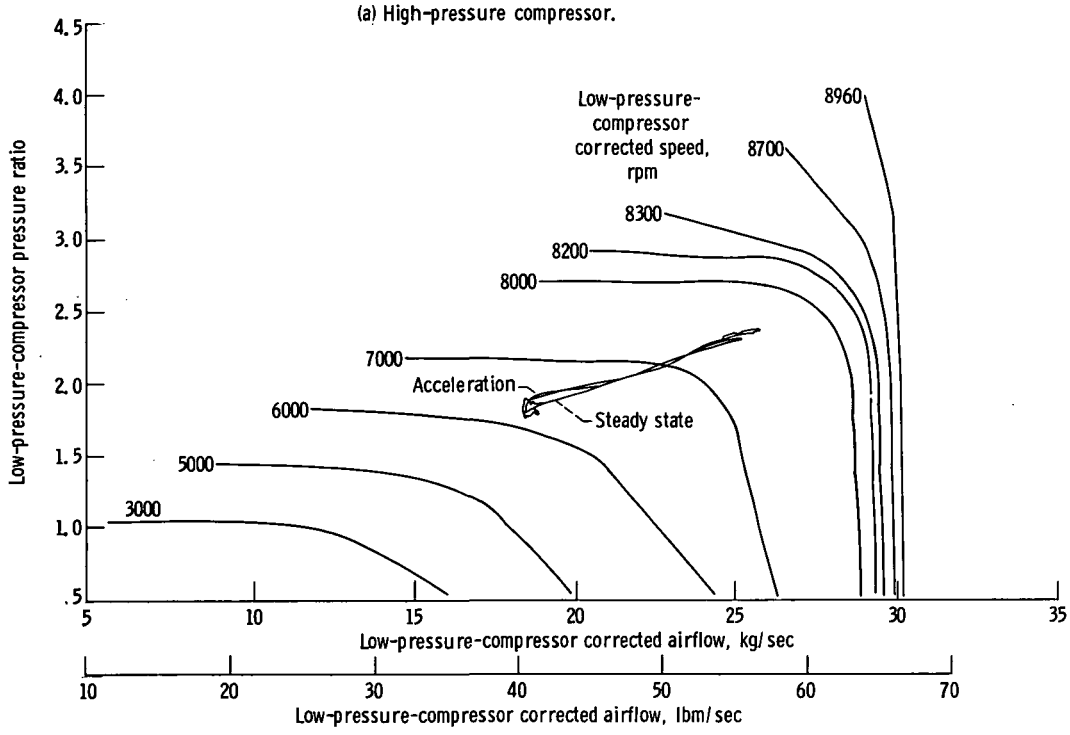

(b) Low-pressure compressor.

Figure 16. - Compressor operating lines for normal operation and for failure of the high-pressure-rotor-speed and high-pressure-compressor-discharge-static-pressure sensors. Flight condition, Mach 1.2 and 3.0-km (10 000-ft) altitude; data obtained at Mach 0.8 and 9.2-km (30 000-ft) altitude.

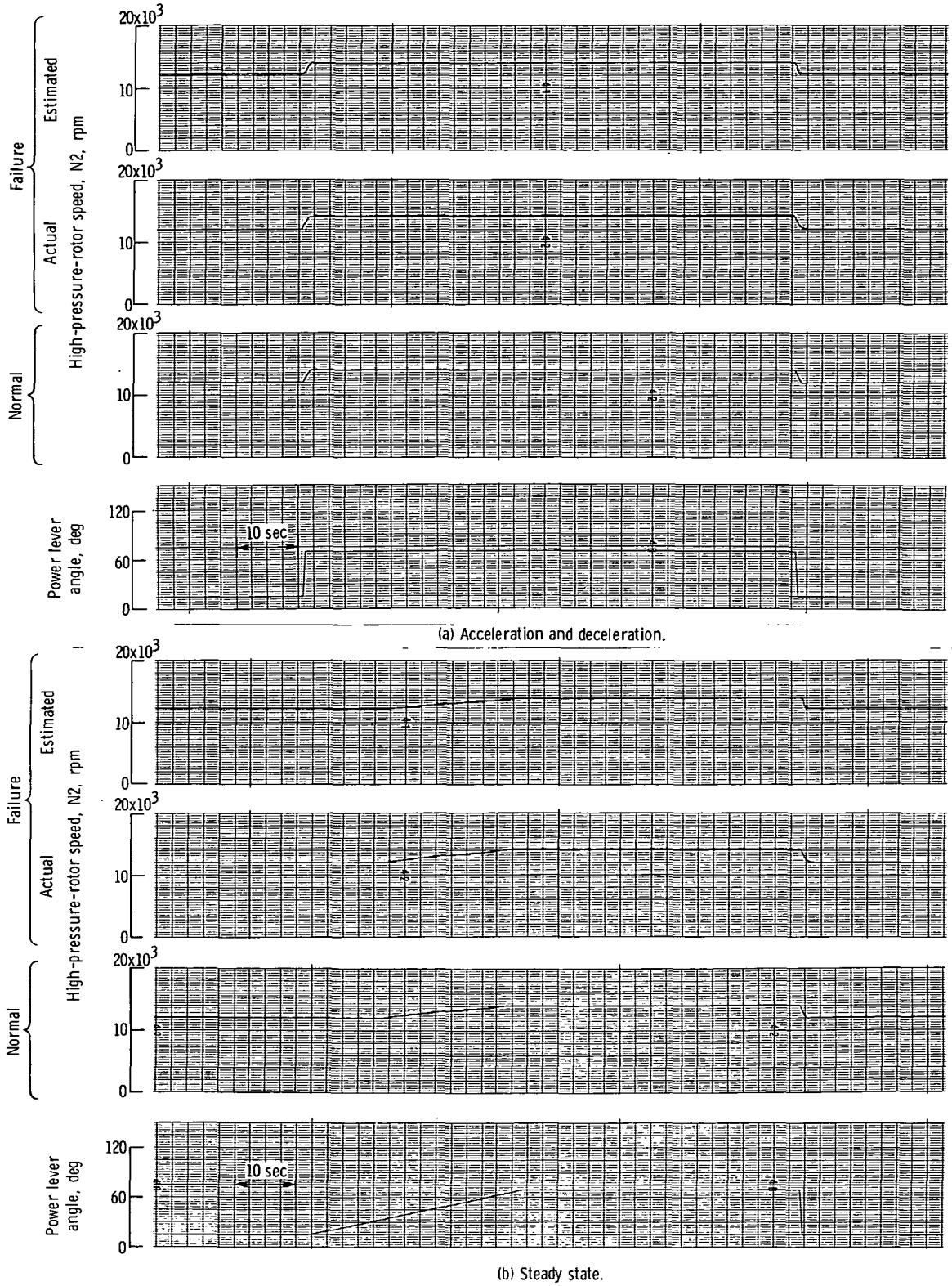

Figure 17. - High-pressure-rotor speed for normal operation and for failure of the high-pressure-rotor-speed and high-pressure-compressor-discharge-static-pressure sensors. Flight condition, Mach 1.2 and 3.0-km (10 000-ft) altitude; data obtained at Mach 0.8 and 9.2-km (30 000-ft) altitude.

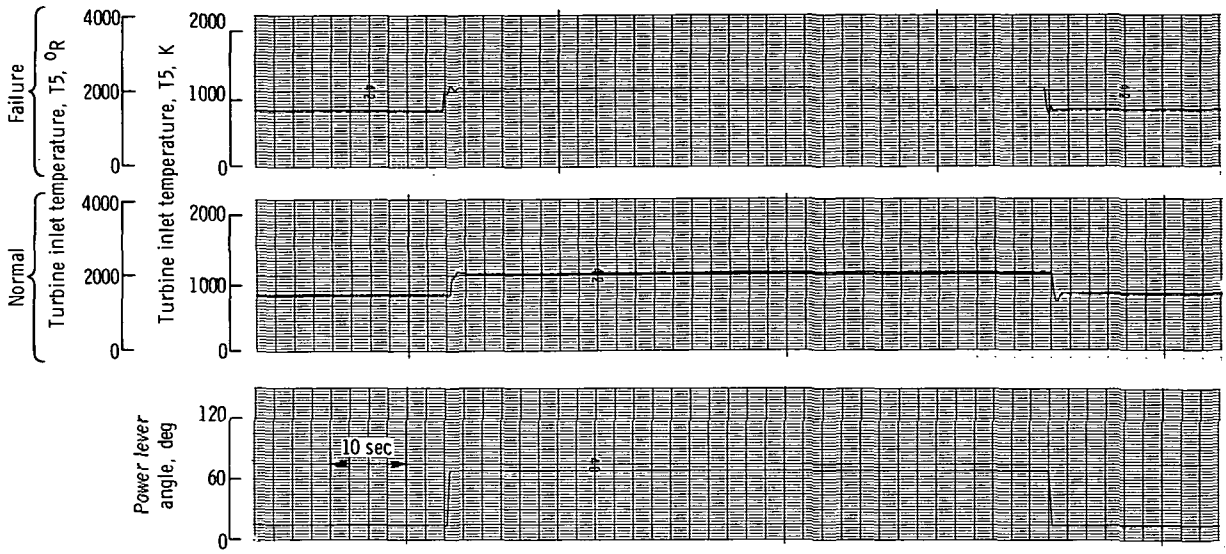

(a) Acceleration and deceleration.

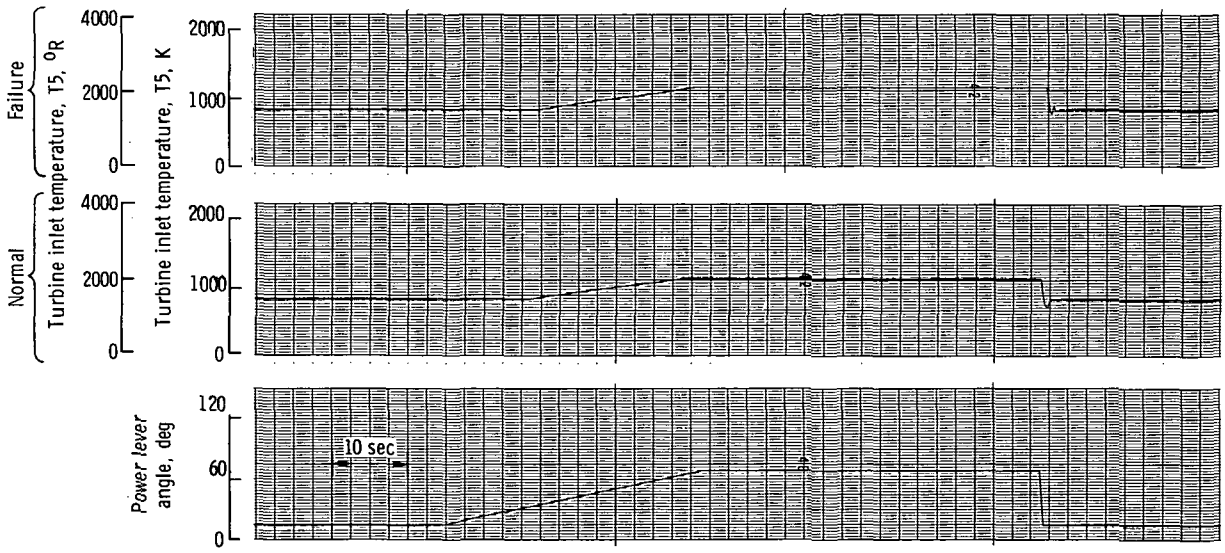

(b) Steady state.

Figure 18. - Turbine inlet temperature for normal operation and for failure of the high-pressure-rotor-speed and high-pressure-compressor-discharge-static-pressure sensors. Flight condition, Mach 1.2 and 3.0-km (10 000-ft) altitude; data obtained at Mach 0.8 and 9.2-km (30 000-ft) altitude.

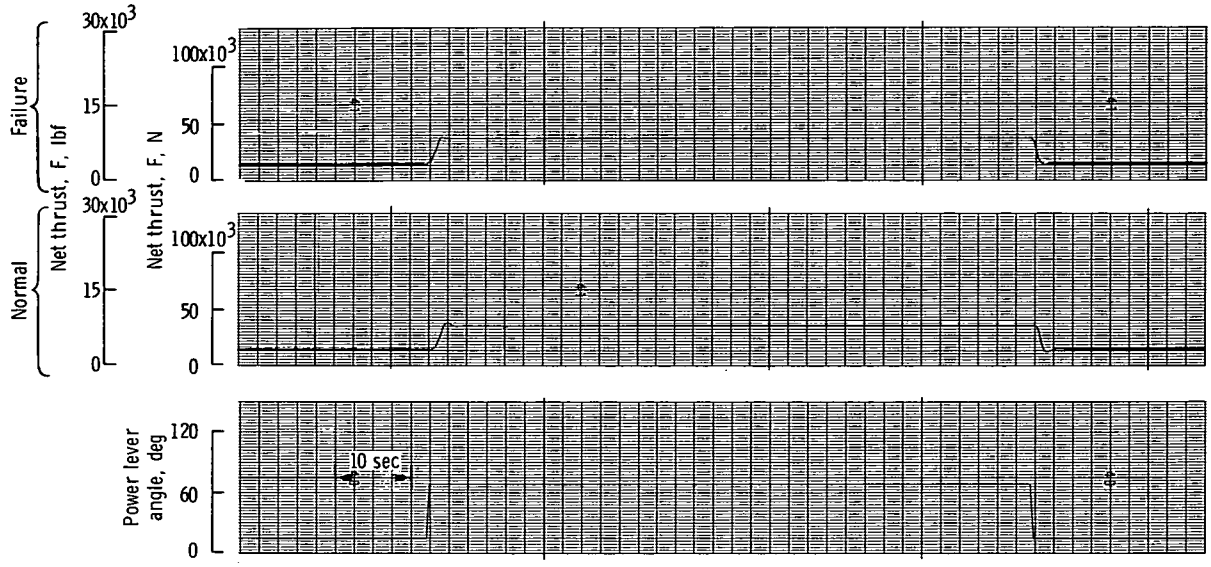

(a) Acceleration and deceleration.

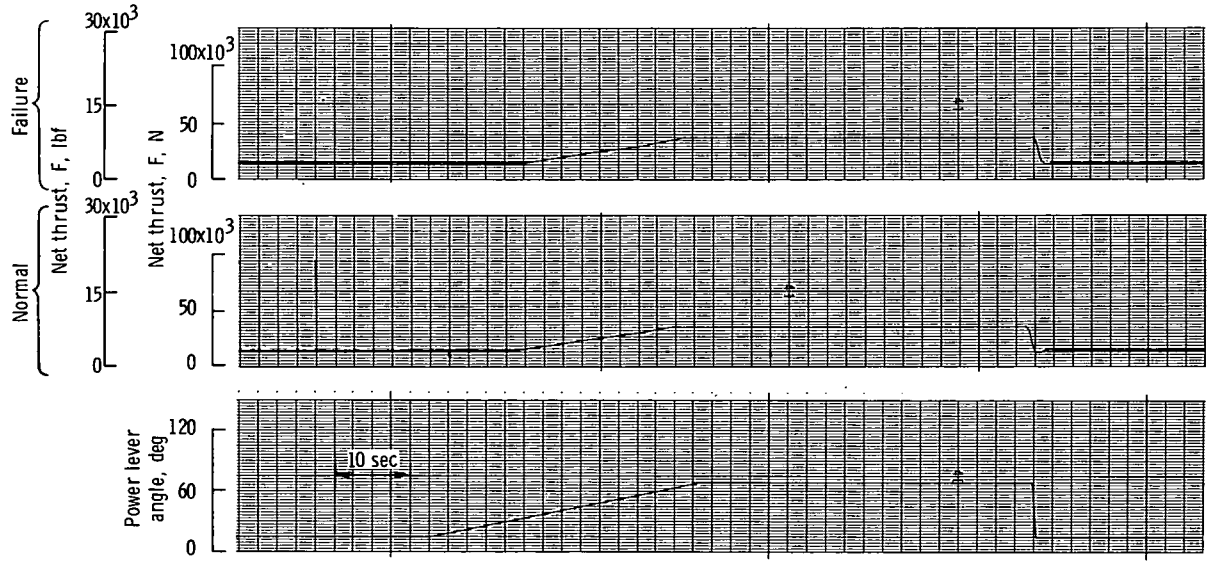

(b) Steady state.

Figure 19. - Net thrust for normal operation and for failure of the high-pressure-rotor-speed and high-pressure-compressor-discharge-static-pressure sensors. Flight condition, Mach 1.2 and 3.0-km (10 000-ft) altitude; data obtained at Mach 0.8 and 9.2-km (30 000-ft) altitude.

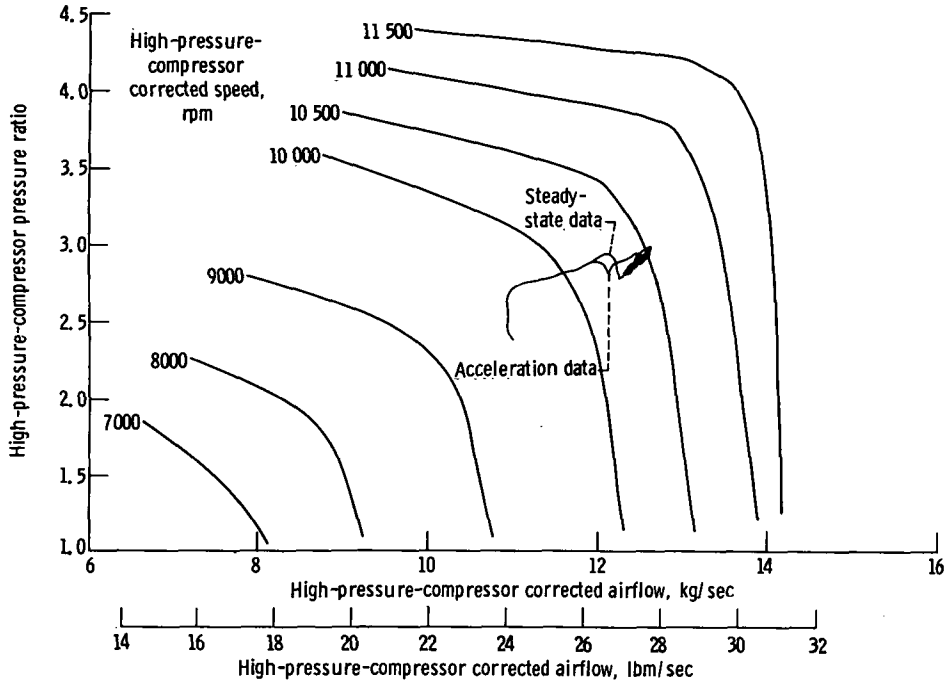

(a) High-pressure compressor.

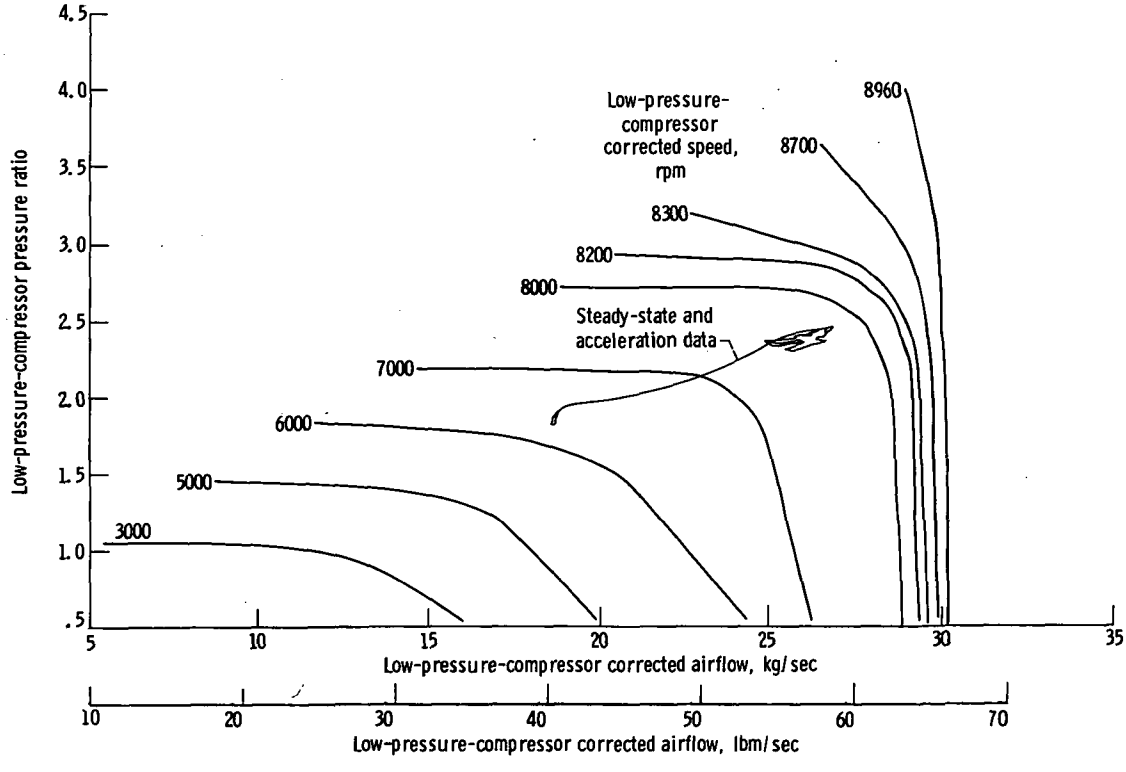

(b) Low-pressure compressor.

Figure 20. - Compressor operating lines for a throttle slam with a high-pressure-rotor-speed sensor failure for the case in which acceleration data are used and for the case in which steady-state data are used. Flight condition, Mach 1.2 and 3.0-km (10 000-ft) altitude; data obtained at Mach 0.8 and 9.2-km (30 000-ft) altitude.

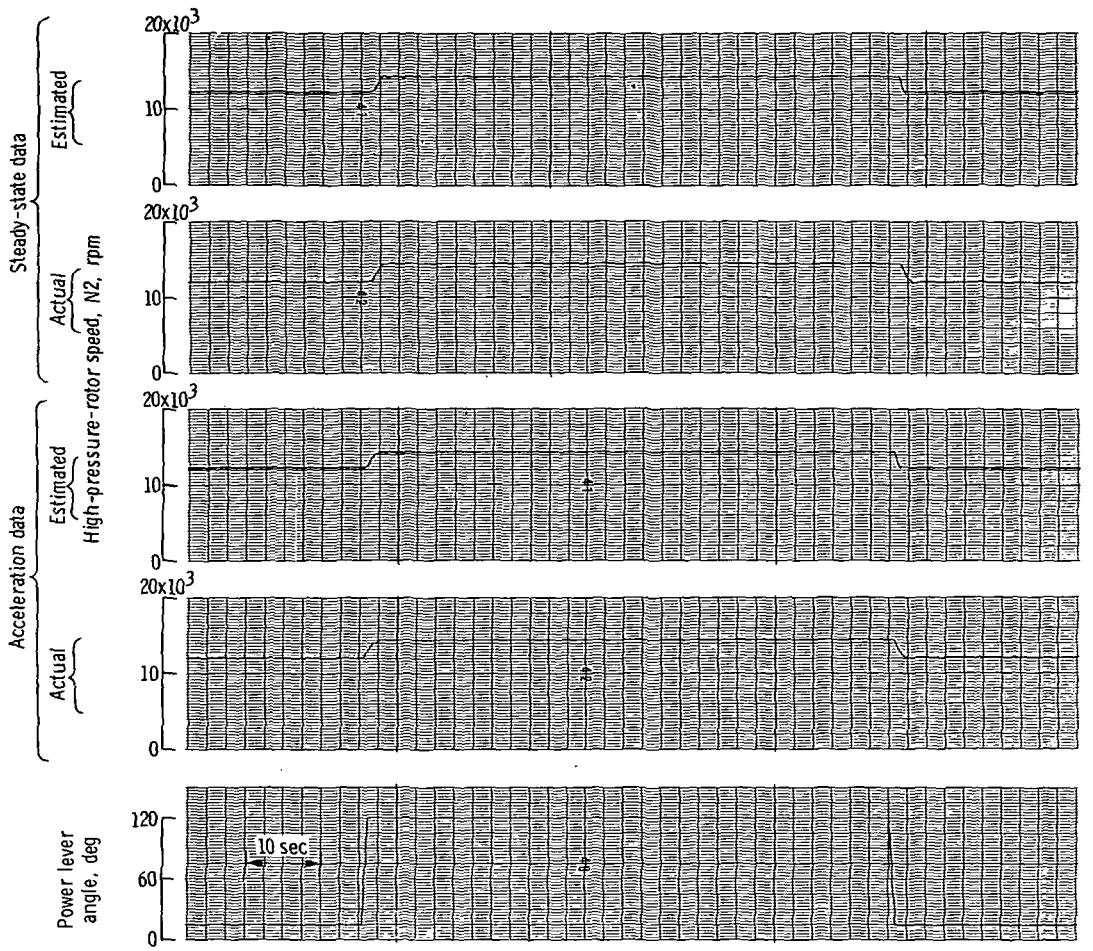

Figure 21. - High-pressure-rotor speed for a throttle slam with a high-pressure-rotor-speed sensor failure for the case in which acceleration data are used and for the case in which steady-state data are used. Flight condition, Mach 1.2 and 3.0-km (10 000-ft) altitude; data obtained at Mach 0.8 and 9.2-km (30 000-ft) altitude.

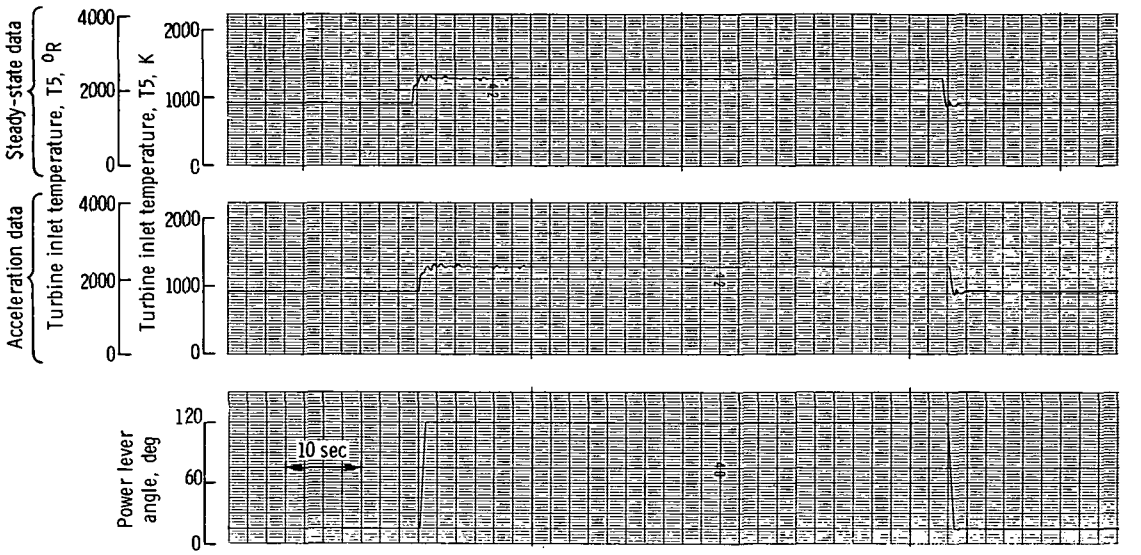

Figure 22. - Turbine inlet temperature for a throttle slam with a high-pressure-rotor-speed sensor failure for the case in which acceleration data are used and for the case in which steady-state data are used. Flight condition, Mach 1.2 and 3.0-km (10 000-ft) altitude; data obtained at Mach 0.8 and 9.2-km (30 000-ft) altitude.

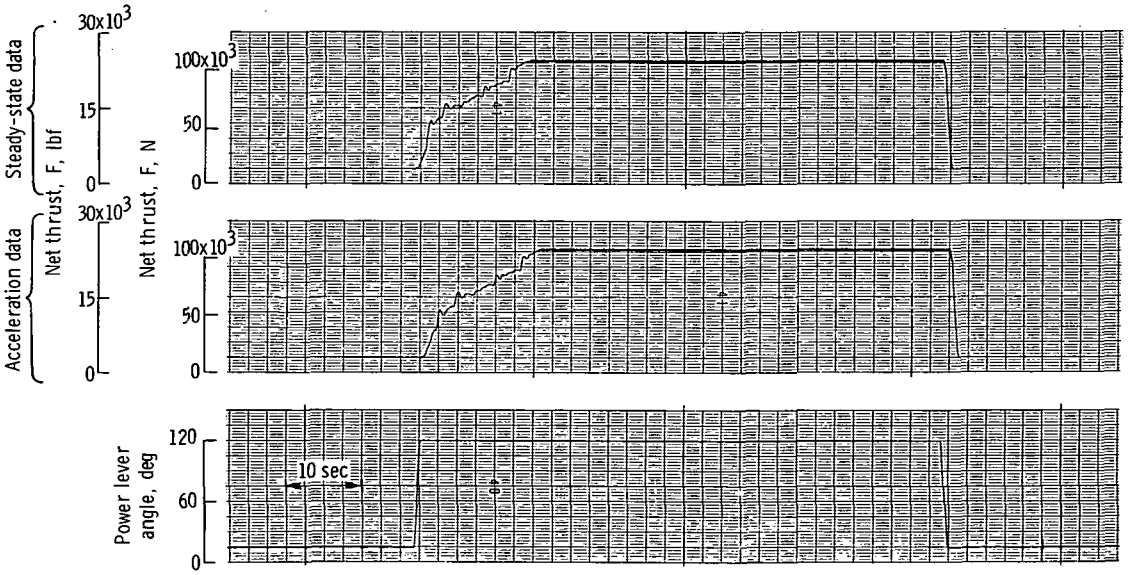

Figure 23. - Net thrust for a throttle slam with a high-pressure-rotor-speed sensor failure for the case in which acceleration data are used and for the case in which steady-state data are used. Flight condition, Mach 1.2 and 3.0-km (10 000-ft) altitude; data obtained at Mach 0.8 and 9.2-km (30 000-ft) altitude.

NATIONAL AERONAUTICS AND SPACE ADMINISTRATION
WASHINGTON, D.C. 20546

OFFICIAL BUSINESS
PENALTY FOR PRIVATE USE $300

SPECIAL FOURTH-CLASS RATE
BOOK

POSTAGE AND FEES PAID
NATIONAL AERONAUTICS AND
SPACE ADMINISTRATION
451

U.S.MAIL

POSTMASTER: If Undeliverable (Section 158 Postal Manual) Do Not Return

"The aeronautical and space activities of the United States shall be conducted so as to contribute . . . to the expansion of human knowledge of phenomena in the atmosphere and space. The Administration shall provide for the widest practicable and appropriate dissemination of information concerning its activities and the results thereof."

—NATIONAL AERONAUTICS AND SPACE ACT OF 1958

NASA SCIENTIFIC AND TECHNICAL PUBLICATIONS

TECHNICAL REPORTS: Scientific and technical information considered important, complete, and a lasting contribution to existing knowledge.

TECHNICAL NOTES: Information less broad in scope but nevertheless of importance as a contribution to existing knowledge.

TECHNICAL MEMORANDUMS: Information receiving limited distribution because of preliminary data, security classification, or other reasons. Also includes conference proceedings with either limited or unlimited distribution.

CONTRACTOR REPORTS: Scientific and technical information generated under a NASA contract or grant and considered an important contribution to existing knowledge.

TECHNICAL TRANSLATIONS: Information published in a foreign language considered to merit NASA distribution in English.

SPECIAL PUBLICATIONS: Information derived from or of value to NASA activities. Publications include final reports of major projects, monographs, data compilations, handbooks, sourcebooks, and special bibliographies.

TECHNOLOGY UTILIZATION PUBLICATIONS: Information on technology used by NASA that may be of particular interest in commercial and other non-aerospace applications. Publications include Tech Briefs, Technology Utilization Reports and Technology Surveys.

Details on the availability of these publications may be obtained from:

SCIENTIFIC AND TECHNICAL INFORMATION OFFICE

NATIONAL AERONAUTICS AND SPACE ADMINISTRATION

Washington, D.C. 20546